Results in Chemistry 5 (2023) 100842

Contents lists available at ScienceDirect

Results in Chemistry

journal homepage: www.sciencedirect.com/journal/results-in-chemistry

Discovery of aminothiazole derivatives as a chemical scaffold for glutaminase inhibition

Renna K.E. Costa [a,b,1], Guilherme A. Brancaglion [c,1], Matheus P. Pinheiro [a], Douglas Adamoski [a], Bianca N. da Silva [a,b], Cyro Z. de V. Negrao [a,b], Kaliandra de A. Gonçalves [a], Camila T. Rodrigues [d], Andre L.B. Ambrosio [d], Rafael V.C. Guido [d], Julio C. Pastre [c,*], Sandra M.G. Dias [a,*]

[a] Brazilian Biosciences National Laboratory (LNBio), Center for Research in Energy and Materials (CNPEM), 13083-100 Campinas, SP, Brazil
[b] Graduate Program in Genetics and Molecular Biology, Institute of Biology, University of Campinas-UNICAMP, Campinas, SP, Brazil
[c] Institute of Chemistry, University of Campinas-UNICAMP, 13083-970 Campinas, SP, Brazil
[d] Sao Carlos Institute of Physics (IFSC), University of Sao Paulo (USP), 13563-120 Sao Carlos, SP, Brazil

ARTICLE INFO

Keywords:
Triple-negative breast cancer
Glutaminase
Cell metabolism
High throughput screening
Enzyme inhibitors

ABSTRACT

Cancer cells rely on different mechanisms to maintain their dysregulated metabolism and high proliferation. Metabolic rewiring with an increased dependency on glutamine, the most abundant amino acid in the blood, is a common feature of several types of cancers, including triple-negative breast cancer (TNBC). The enzyme glutaminase (GLS) converts glutamine to glutamate, a reaction that provides α-ketoglutarate for the tricarboxylic/citric acid cycle (TCA) and chromatin-modifying enzymes, thus impacting proliferation and cell differentiation. Glutamine metabolism also impacts the redox balance and synthesis of nucleotides, lipids, and other amino acids. Glutaminase is a potential therapeutic target for cancer, with inhibitors in clinical trials. We previously performed high-throughput screening (HTS) to look for GLS inhibitors. Here, we present the structure–activity relationship (SAR) study of one of the hits, C12, a molecule containing the heteroaromatic nucleus 2-amino-thiazole. The SAR investigation was carried out through modifications of the substituents from the main 3 rings present at the C12 prototype, rings A-C. The combination of 4-F and phenylacetic substitutions on ring A, the incorporation of a 1,3,4-thiadiazole moiety on ring B, and a 4-CN substituent on ring C were the best options to improve specific GLS inhibition. In this series, three compounds exhibited suitable enzyme (GAC vs GLS2) and cell (MDA-MB-231 vs SKBR3) selectivity and, thus, could be useful for the development of new glutaminase inhibitors.

Introduction

Metabolic reprogramming is one of the hallmarks of cancer cell transformation [1–2] and is linked to the dysregulated nutrient uptake needed to satisfy the biosynthetic and redox requirements for cell survival and proliferation [3–4]. The increase in glucose uptake and its metabolism to generate lactate, even in the presence of oxygen – known as the Warburg effect [5], – is often associated with an increased dependency on the amino acid glutamine; together, glucose and glutamine provide carbon and nitrogen for the Tricarboxylic Acid Cycle (TCA), which become a source for biosynthetic intermediates that are used for biomass duplication in addition to producing reducing equivalents for the electron transport chain and ATP synthesis [6–7]. GLS promotes the hydrolytic deamination of glutamine to glutamate [8], the first step in the catabolism of this amino acid, which is converted to the metabolite α-ketoglutarate by the enzyme glutamate dehydrogenase (GDH) or transaminases [9–10]. This metabolite is a key cofactor for chromatin-modifying histone demethylases and is used to block cell differentiation epigenetically [11].

Mammalian glutaminases are encoded by two different but related genes [12–13]. The *GLS* gene is alternatively spliced into glutaminase C (GAC) and kidney-type glutaminase (KGA) [14–15]. *GLS2* codes for

* Corresponding authors.
E-mail addresses: jpastre@unicamp.br (J.C. Pastre), sandra.dias@lnbio.cnpem.br (S.M.G. Dias).
[1] These authors contributed equally.

https://doi.org/10.1016/j.rechem.2023.100842
Received 28 January 2023; Accepted 6 February 2023
Available online 10 February 2023

glutaminase B (GAB) and liver-type glutaminase (LGA) through the use of alternative transcription initiation sites [16]. GAC is the most catalytically active glutaminase isoform and forms long filaments in the presence of the activator inorganic phosphate (Pi) [17].

TNBC accounts for approximately 15% of breast cancer cases [18–19] and shows a worse prognosis, higher recurrence rate and more aggressiveness than other breast cancer subtypes [20–21]. TNBC is well known for the lack/nondetection of the estrogen receptor (ER) and progesterone receptor (PR) and the expression of normal levels of HER2, causing TNBC to be nonresponsive to hormonal and other more efficient targeted therapies, leaving cytotoxic chemotherapies as the only resort [22–23]. We and others have previously shown that GAC levels are increased in breast cancer, and is therefore, a promising therapeutic target for this disease [15,24–25]. The search for GLS inhibitors dates back to the 1950s and has not yet come to an end [20].

The first allosteric GLS inhibitor described was bis-2-(5-phenylacetamido-1,2,4-thiadiazol-2-yl)ethyl sulfide (BPTES) [21], which leads to the formation of a stable but inactive tetramer of this enzyme [26–28]. Despite its high potency, BPTES has low bioavailability, making its use unfeasible in the clinic but opening the possibility for medicinal chemistry exploration [29–30]. Along this line, two BPTES-derived compounds have entered clinical trials, CB-839 [31–32] and IPN60090 [33]. CB-839 and IPN60090 show the same inhibition mechanism but display improved potency and pharmacokinetics behavior compared to BPTES [31,33]. Finley and coworkers also developed their own BPTES/CB-839 derivative, which showed better pharmacokinetics and oral bioavailability during preclinical trials [34]. Additionally, Xu and coworkers developed a 31-atom macrocyclic compound with an IC_{50} of 6 nM [34]. This compound is also a CB-839 derivative, but its extremities are linked by a 6-carbon chain that causes some conformational constraints, which accounts for its improved inhibition [34]. Aside from these molecules, several others have already been proposed and exhibited modest activities [29–30,35–36].

We previously published the results of an HTS campaign using a diverse collection of ~30,000 small molecules [17]. In this work, we evaluate 12 hits and 21 analogues and present the SAR analysis of the hit of interest (C12), a molecule with the heteroaromatic 2-amino-thiazole nucleus. Synthetically, 2-aminothiazoles are easily accessible heterocycles that can be obtained via a Hantzsch's thiazole synthesis reaction between any kind of thiourea and an α-halo ketone or aldehyde in refluxing ethanol [37]. The substitution pattern of the aminothiazole ring can be modified depending on the kind of α-halo carbonyl compound used in the synthesis. Ketones can produce either C4 only- or both C4- and C5-substituted 2-aminothiazoles, while aldehydes produce C5-substituted rings. Both reagents in this reaction are also easily generated [38]. The thiourea can be prepared by reaction of an amine or aniline with thiocyanate salts in acidic medium [39–40]. Most of the α-halo carbonyl compounds can be prepared by reacting a ketone with copper(II) bromide or with NBS in a HBr solution. These compounds can also be directly prepared through Friedel-Crafts acylation with chloroacetyl chloride. Acetaldehydes can be brominated using L-proline and NBS in DCM [41].

Our work explores a novel scaffold for generating selective GAC inhibitor molecules and shows their synthetic routes. The aminothiazoles have an easily accessible synthetic procedure when compared to larger GLS inhibitors, like CB-839 and IPN60090. The derivatives presented in this work show an IC_{50} in the low micromolar range with a considerably smaller structure and molecular weight, which could provide suitable bioavailability properties. Even though there are others GLS inhibitors with low nanomolar IC_{50} values, they have yet to complete clinical trials. Thus, a commercial drug targeting GLS inhibition is still pending. Bearing this in mind, our purpose is to present a smaller new moiety for GLS inhibitors that may contribute to future research in the field.

Results and discussion

Cell-based and biochemical glutaminase inhibition assays

TNBCs exhibit high glutaminase expression and low glutamine synthetase expression [19]. This expression pattern is associated with high glutamine consumption and exogenous glutamine-dependent growth. Indeed, TNBCs are more sensitive to glutaminase inhibition than non-TNBC subtypes [31]. We used the MDA-MB-231 TNBC cell line, which exhibits high GAC expression, as a model to evaluate the responses produced by the 33 compounds on cell proliferation, using CB-839 as a positive control. Moreover, the inhibitory effects of the compounds were evaluated in a non-TNBC cell line, SKBR3, which is known for its low GAC expression [19].

All 33 compounds (**Figure S1**) were supplied by ChemBridge, diluted in DMSO, and incubated with the cells for 72 h at a concentration of 10 μM. The compound CB-839 was used as a positive control, and DMSO was used as a negative control. As expected, CB-839 inhibited MDA-MB-231 growth by 80% (Fig. 1**A**, Table 1, **and Table S1 for complete data),** but very little SKBR3 growth inhibition was observed (2.3%) (Fig. 1**B**, Table 1). Two molecules, C15.1 (an analog of hit C15) and C12, showed the most pronounced effect on MDA-MB-231 cells, with 38.4 ± 3.9% and 22.9 ± 4.8% growth inhibition, respectively (Fig. 1**A**, Table 1 **and Table S1**). On the other hand, compounds C15.1 and C12 inhibited SKBR3 cell growth by 28.4 ± 1.5% and 3.9 ± 0.2%, respectively (Fig. 1**B**, Table 1 **and Table S1**). The fold inhibition of MDA-MB-231 compared to SKBR3 cells was 1.4 for C15.1 and 5.9 for C12 suggesting that C12 may be more selective than C15.1 (Table 1 **and Table S1**).

Accordingly, dose–response assays with C12 and C15.1 in MDA-MB-231 cells investigating growth inhibition revealed IC_{50} values of 24.7 (confidence interval 95%, CI95%, 22.8–26.8) μM and 26.9 (24.7–29.1) μM, respectively. C15 and its analogue C15.2 displayed IC_{50} values of 78.2 (73–84.6) μM and 53.8 (48.6–59.2) μM, respectively (Fig. 1**C**). The chemical structures of compounds C12, C15, C15.1 and C15. 2 are displayed in Fig. 1**D**.

Next, we evaluated a single dose of all 33 compounds (10 μM) using an absorbance assay [10,42]. The tested compounds decreased the activity of the GAC enzyme by 1.6 ± 3.2% (C15.2) to up to 98.7% ± 1.2% (C15.1). C12 inhibited 65 ± 1.9% of the GAC activity (Fig. 2**A**, Table 2 **and Table S2**).

We next verified whether compounds C12 and C15.1 could affect GAC activity through a nonspecific aggregation effect. The protein was incubated with the solvent DMSO, the positive control CB-839, or C12 or C15.1. After that, we analysed their dynamic light scattering signals. Each experiment was carried out under two conditions: one contained 500 mM NaCl, which is known to generate a 5–6 nm hydrodynamic radius that is equivalent to the protein in a tetrameric state [17,43], and a second condition with 150 mM NaCl and 20 mM Pi, which leads to filamentation of the tetramers [17,43]. We have previously shown that BPTES and CB-839 inhibit GAC by causing disassembly of the filaments to generate inactive tetramers [17,43].

Interestingly, in 500 mM NaCl, CB-839, C12, and C15.1 stabilized the protein in a tetrameric state (6 ± 1 nm hydrodynamic radius, r; Fig. 2**B**, right). Moreover, in a 150 mM NaCl and 20 mM Pi solution, we observed an increase in the r value to more than that in the tetrameric state, as expected (474 ± 30 nm) (Fig. 2**B**, left, Table 3). CB-839 caused the radius to be 6 ± 1 nm, indicating the tetrameric state, as expected [44–45] (Fig. 2**B**, left, Table 3). On the other hand, C12 and C15.1 did not disassemble the filaments, as they produced radii of 1371 ± 173 and 825 ± 65 nm, respectively. The thermal shift assay showed that both C12 and C15.1 stabilize the enzyme since they increased the melting temperature by 2.5 °C and 2.3 °C, respectively, in the presence of Pi (but not in its absence) (Fig. 2**C**). Combining the cellular and enzymatic potency data, we chose C12 for the SAR study.

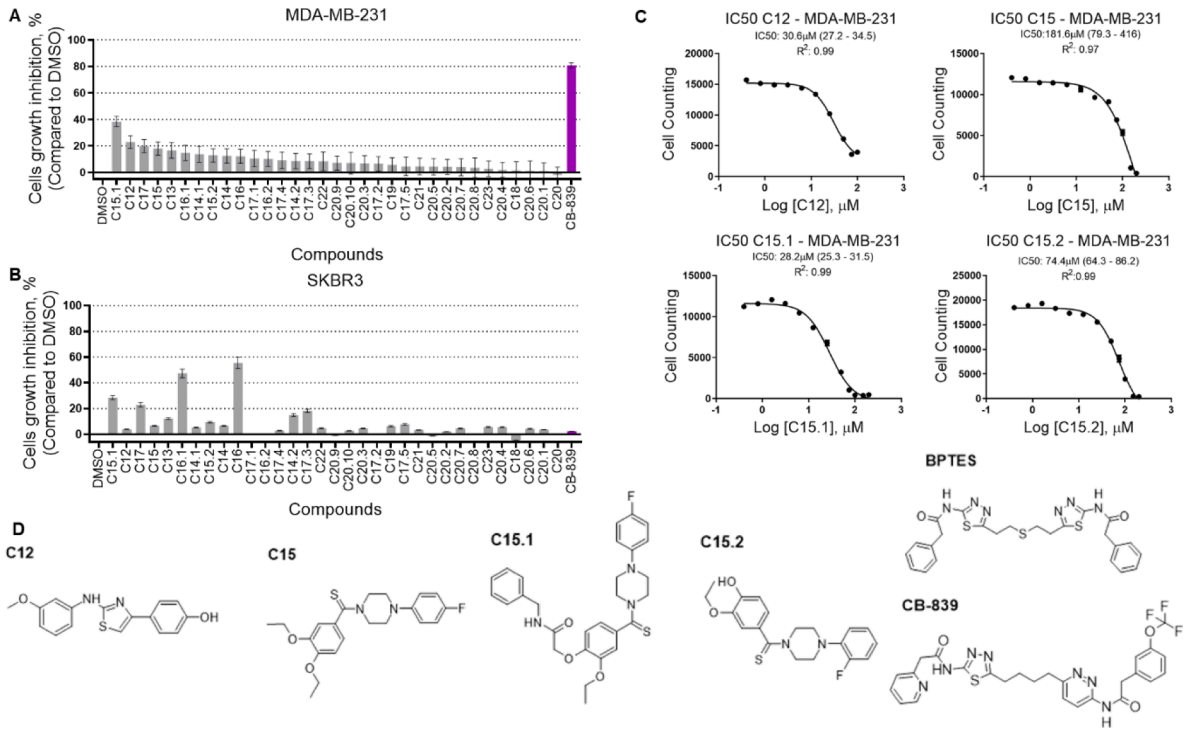

Fig. 1. Effects of the compounds on MDA-MB-231 and SKBR3 cell growth. Inhibition of TNBC MDA-MB-231 (A) and SKBR3 (B) cell proliferation producedby a single concentration of each of the 33 evaluated compounds (10 μM) and CB-839 (1 μM). DMSO was used at a concentration of 0.1%. Averages and standard deviations (SDs) are presented. (C) IC_{50} values of C12, C15, C15.1 and C15.2 to inhibit MDA-MB-231 cell growth. (D) Chemical structures of C12, C15, C15.1, C15.2, BPTES and CB-839.

Table 1
Inhibitory activity of C12, C15, C15.1 and C15.2 in MDA-MB-231 and SKBR3 cells.

Compounds	ID# Chembridge	% Inhibition MDA-MB-231 (10μM)		% Inhibition SKBR3 (10μM)		Fold inhibition (% Inhibition MDA-MB-231/ %Inhibition SKBR3)
		% Inhibition	SD	% Inhibition	SD	
C12	7,874,229	22.9	4.8	3.9	0.2	5.9
C15	7,943,337	18.0	5	6.5	0.4	2.8
C15.1	7,775,987	38.4	3.9	28.4	1.5	1.4
C15.2	7,747,354	12.8	0.7	9.4	0.6	1.4

Chemical synthesis of the C12 derivatives

Scheme 1 shows the **C12** prototype regions that were investigated during the SAR evaluation (**A**) and the microwave assisted Hantzsch's aminothiazole synthesis reaction that was utilized to obtain the derivatives (**B**). This reaction allowed quick access to the desired 2-aminothiazole series by just selecting the thiourea or the α-halo carbonyl intermediates that were used in the procedure. The thioureas were prepared beforehand, and some of the α-halo carbonyl intermediates were synthesized, even though they are commercially available. The synthetic procedures for the different phenylthiourea intermediates (**1a-1l**) and for the α-halo carbonyl intermediates (**2a-2g** and **2p**) that needed to be synthesized are presented in the SI.

Six derivatives needed additional reactions or a different approach to be prepared (Scheme 2). To synthesize **C12.16**, the aromatic nitro group present in derivative **C12.4** was reduced to an aniline using tin(II) chloride in refluxing ethanol, leading to intermediate **3a**. Then, the resulting aniline was combined with phenylacetyl chloride (**4a**) to form an amide (Scheme 2, A).

For the synthesis of derivative **C12.17**, 2-amino-4-phenylthiazole (**3b**) was synthesized in a reaction between thiourea and 2-bromoacetophenone (**2h**) using Hantzsch's procedure. Then, **3b** and phenylacetic acid **4b** were combined through EDC- and DMAP-mediated amide synthesis. Derivative **C12.31** was obtained in a similar manner, but by exchanging 2-bromoacetophenone for 2-bromo-4′-cyanoacetophenone (**2a**) to form **3c** and phenylacetic acid for 4-fluorophenylacetic acid (**4c**) to form **C12.32** (Scheme 2, B).

The 5C-substituted aminothiazole moiety in derivative **C12.18** was synthesized by using 2-bromo-2-phenylacetaldehyde (**2q**), which was prepared from 2-phenylacetaldehyde (**4d**) and readily used (Scheme 2, C).

For the synthesis of derivative **C12.33**, an S_N2 reaction was carried out between 5-amino-1,3,4-thiadiazole-2-thiol (**4e**) and 4-(bromomethyl)benzonitrile (**4f**) to form intermediate **3d**. Then, this intermediate was subjected to an acylation reaction with 4-fluorophenylacetic acid (**4c**) mediated by EDC and DMAP (Scheme 2, D). Derivative **C12.34** was synthesized in a similar manner but with an additional step to obtain alkylating agent **3e** (Scheme 2, E). First, 4-aminobenzonitrile (**4g**) was acylated with bromoacetyl bromide (**4h**) to form intermediate **3e**, and then the alkylation reaction was carried out with **3e** and 5-amino-1,3,4-thiadiazole-2-thiol (**4e**) to form **3f**. Finally, **3f** was acylated with 4-fluorophenylacetic acid (**4c**) to form **C12.34**.

Structure-activity relationship studies of C12 and its derivatives

The SAR study investigating the ability of C12 to inhibit the enzyme GAC was carried out by synthesizing derivatives with different substituents throughout the main 3 regions of this compound (Scheme 1). It

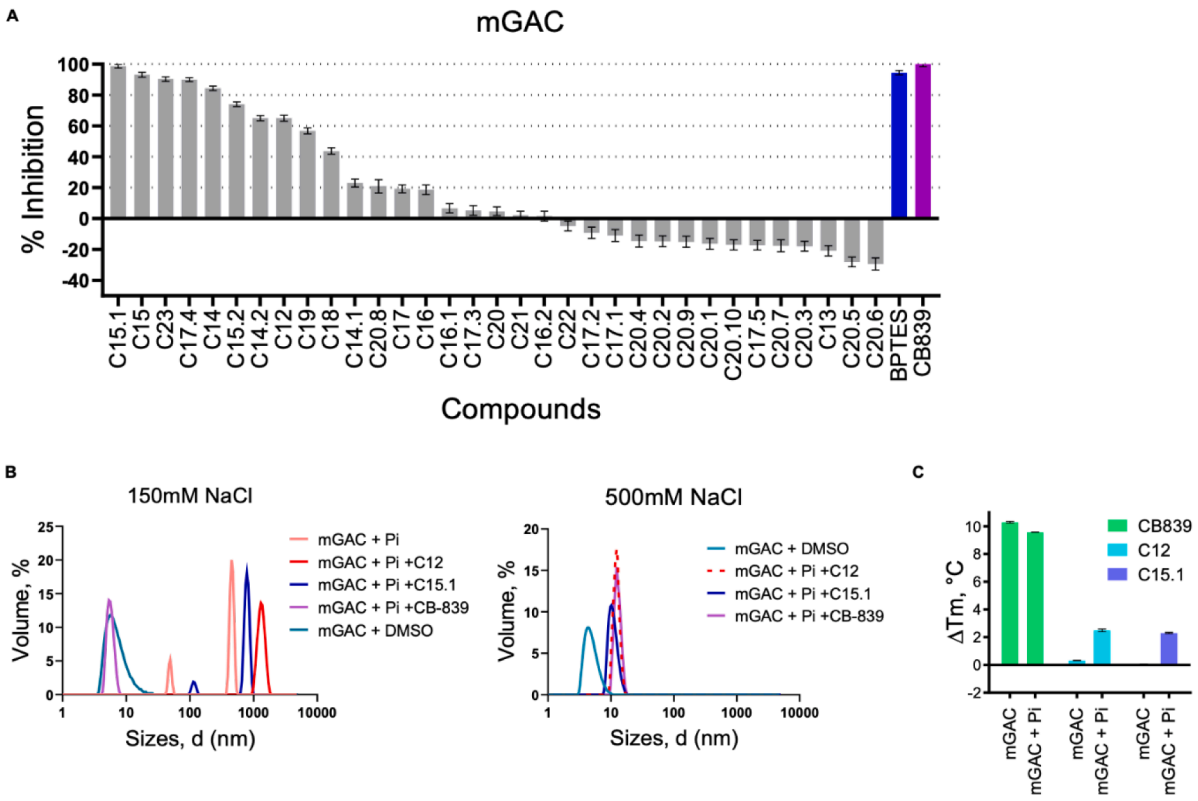

Fig. 2. The inhibitory properties of the compounds on GAC. Percent GAC (A) inhibition by the compounds and CB-839. (B) Dynamic light scattering of GAC incubated with a solution containing 150 mM NaCl (left) and 500 mM NaCl (right) shows that C12 and C15.1 (both at 200 μM) are not capable of disassembling the activated glutaminase filaments [17,25] (left) and do not cause nonspecific aggregation (right). CB-839 (1 μM) was used as a positive control, and DMSO (0.1%) was used as a negative control. (C) Thermal shift assay shows that both C12 and C15.1 (10 μM) can stabilize GAC in the presence of the enzyme activator Pi. CB-839 (1 μM) was used as a positive control.

Table 2
% GAC inhibitory activity of C12, C15, C15.1 and C15.2.

Compounds	ID #Chembridge	% Inhibition GAC (10μM)	
		% Inhibition	Standard Deviation
C12	7,874,229	65.0	1.9
C15	7,943,337	93.2	1.6
C15.1	7,775,987	98.7	1.2
C15.2	7,747,354	74.1	1.5
CB-839	N/A	100	1.8

Table 3
Dynamic light scattering analysis of the tested samples and control (DMSO).

Solution	Compound	Size Peak (r.nm) ±SD[§]	Volume, %	Polydispersity, %
500 mM	DMSO	6 ± 1	100	47.6
NaCl	C12	6 ± 1	98.8	76.4
	C15.1	6 ± 2	100	40.3
	CB-839	6 ± 1	100	66.7
150 mM	DMSO	474 ± 30	82.3	100
NaCl	C12	1371 ± 173	100	48.4
+20 mM	C15.1	825 ± 65	92	88.4
Pi	CB-839	6.2 ± 0.8	100	64.6

[§] Mode and standard distribution (SD) of one technical replicate representative of three replicates is presented.

is also important to note that replacements meant to reduce C12 activity toward the GDH enzyme were also considered, as this enzyme was also used in the GAC inhibition assay and is present during glutamine metabolism.

Modifications to ring A (Table 4**)** at both the *meta* and *para* positions involving smaller substituents than the original 3-OMe group (**C12**: GAC IC_{50} 44 μM) showed higher inhibitory activity toward GAC. Substituents such as 4-Me (**C12.14**: GAC IC_{50} 4 μM), 4-F (**C12.15**: GAC IC_{50} 8 μM), 3,5-bis CF_3 (**C12.3**: GAC IC_{50} 12 μM) and H (**C12.12**: GAC IC_{50} 15 μM) afforded compounds with better GAC inhibition. Additionally, except for **C12.3** (GDH inhibition 82%), all of these compounds exhibited lower GDH inhibition than **C12** (GDH inhibition of 81%).

All other replacements on ring A **(**Table 4**)**, including 4-COOH, Phenylacetic, 2-OMe, 4-OMe, 3,4,5-$(OMe)_3$, 4-Cl, and 4-$COCH_3$, resulted in compounds that were only slightly more active or less selective than **C12**. Based on these findings, we decided to keep the 4-F substituent on ring A while modifying the other portions of the parent molecule.

Regarding the exploration of ring C **(**Table 5**)**, the phenol group seemed to be the major contributor to both inhibitory activities, particularly to GDH inhibition. Indeed, all other substituents tested were significantly less active toward GDH than the phenolic group. The presence of a group at any position of ring C that can be a hydrogen bond acceptor appears to be beneficial to GAC activity while maintaining low GDH inhibition (**C12.20**, **C12.19**, **C12.16**, **C12.23** and **C12.29**). Strong, smaller electron withdrawing groups on ring C, such as 4-CN in **C12.19** (GAC IC_{50} 26 μM, GDH inhibition 1.5%) and 4-CF_3 in **C12.23** (GAC IC_{50} 38 μM, GDH inhibition 8.8%), greatly diminished the activity toward GDH while also improving GAC inhibition in comparison to C12 and C12.15, respectively. In addition to the improved inhibitory activity and selectivity toward GAC, these results are even more interesting considering that electron withdrawing groups in a position that can resonate with the aminothiazole ring can also improve 2-aminothiazole metabolic stability [46]. Other electron withdrawing groups on ring C were far less active toward GAC, probably because of their larger volume, like

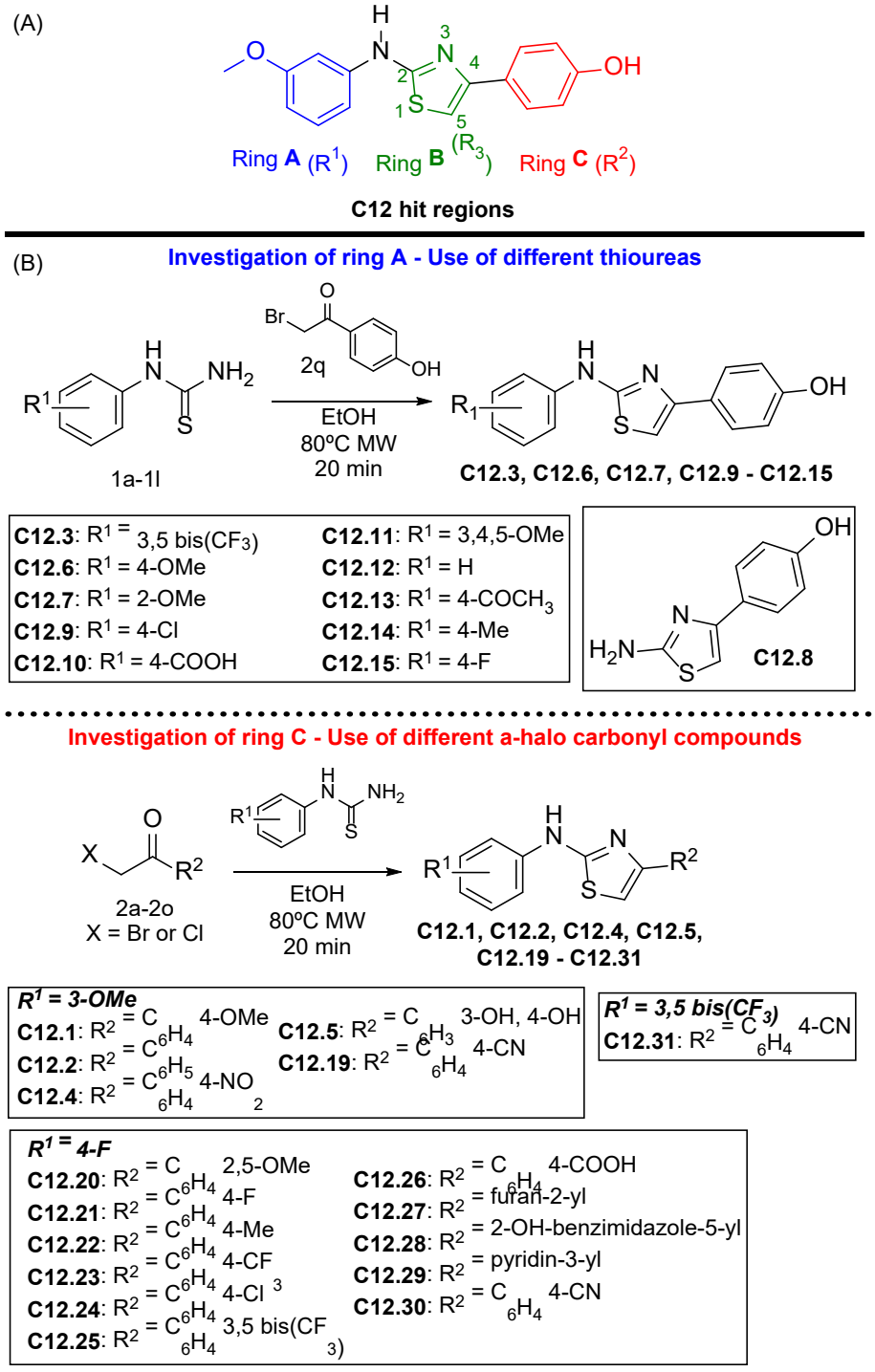

Scheme 1. Synthesis of derivatives **C12.1** - **C12.15** and **C12.19** - **C12.31**.

4-NO_2 (**C12.4**: GAC IC_{50} 99 μM) and 4-COOH (**C12.26**: GAC IC_{50} > 200 μM). Strong electron-donating groups in the *ortho* and *meta* positions of ring **C** appeared to raise the activity, like 2,5-OMe (**C12.20**: 19 μM). Extending the molecule with a phenylacetic moiety on ring C (**C12.16**: GAC IC_{50} 36 μM, GDH inhibition 14.2%) increased the activity against GAC and lowered GDH inhibition in comparison to **C12**.

Next, benzene ring bioisosteres that present better water solubility and that could act as hydrogen bond acceptors were tested. A furan ring in the place of ring C (**C12.27**: GAC IC_{50} 132 μM) was not very active. In turn, a pyridine ring (**C12.29**: GAC IC_{50} 48 μM) showed nearly the same activity as **C12**, even without any substituent. Last, 2-hydroxybenzimidazole was tested as a phenol bioisoster (**C12.28**: GAC IC_{50} 73 μM); however, the GAC activity decreased nearly 10-fold in comparison to **C12.15** (GAC IC_{50} 8 μM). The cyano group on ring C was maintained in these last derivatives because it was shown to be more active toward GAC than **C12** and more selective toward GDH.

The last five derivatives (Table 6) were planned and synthesized by combining the better substituents that were found for ring A (4-F, 3,5-CF_3 and the phenylacetic moiety) and ring C (4-CN). Additionally, the use of a different heterocycle for ring B was explored, which could combine the C5 position at the central ring with the better substituents on the other two rings. This second heterocycle (5-amino-1,3,4-

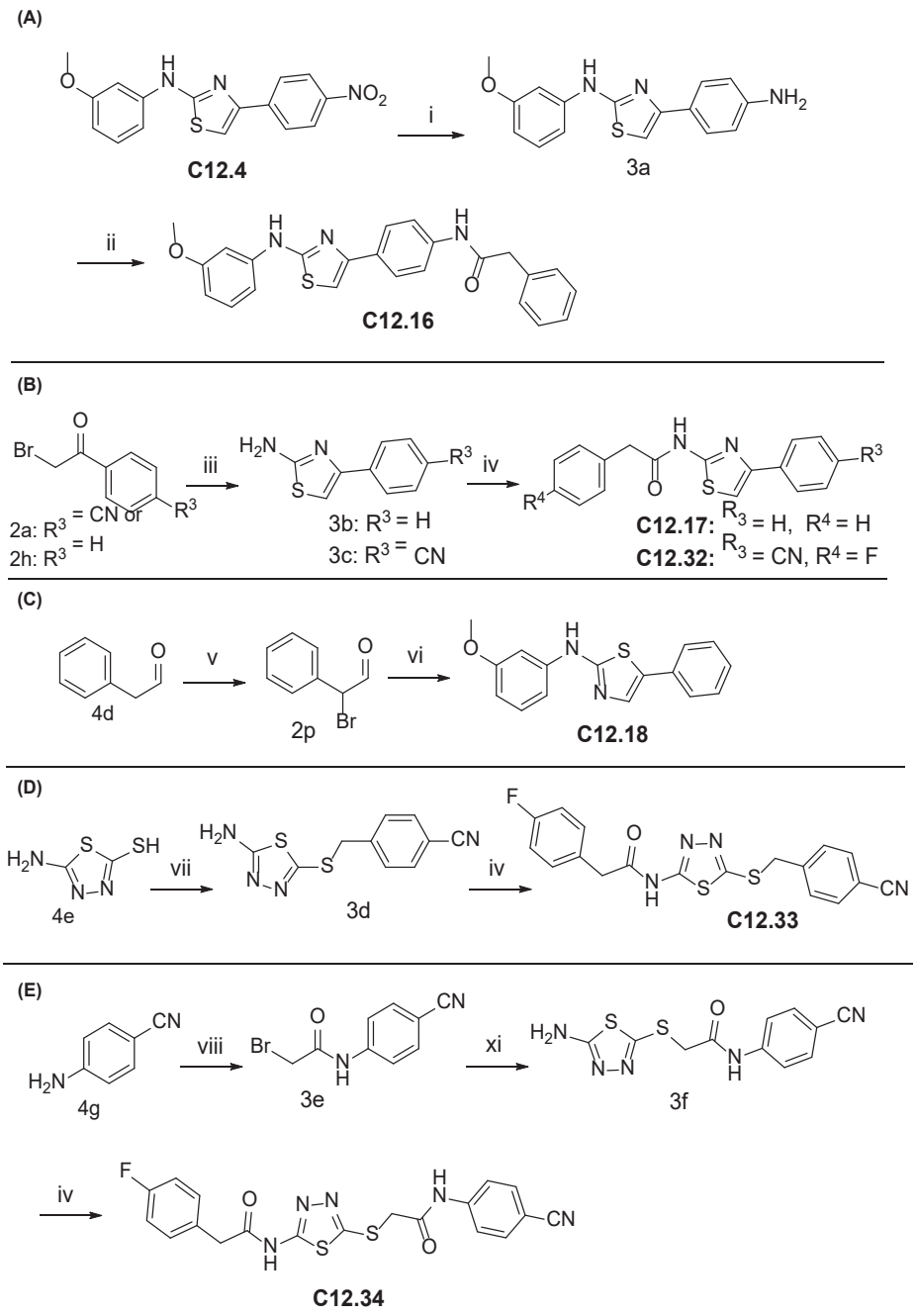

Scheme 2. Synthesis of derivatives **C12.16**, **C12.17**, **C12.18** and **C12.32** – **C12.34**. Reaction conditions: (i) $SnCl_2{\cdot}2H_2O$, EtOH, reflux, 3 h; (ii) phenylacetyl chloride (4a), TEA, THF, r.t., 8 h; (iii) thiourea, EtOH, 80 °C (MW), 0.25 h; (iv) phenylacetic acid (4b) or 4-fluorophenylacetic acid (4c), EDC, DMAP, THF, r.t., 18 h; (v) NBS, (*S*)-proline, DCM, r.t., 3 h; (vi) *N*-(3-methoxyphenyl)thiourea (1a), EtOH, 80 °C (MW), 0.25 h; (vii) 4-(bromomethyl)benzonitrile (4f), K_2CO_3, MeCN, r.t., 16 h; (viii) bromoacetyl bromide (4 h), TEA, dry CH_2Cl_2, 0 °C - r.t., 3 h; (xi) 5-amino-1,3,4-thiadiazole-2-thiol (4e), K_2CO_3, DMF, r.t., 24 h.

thiadiazol-2-thiol) is similar to the one present in BPTES and CB-839 and could allow the evaluation of how the improved substitutions found for the 2-aminothiazole would behave in a different scaffold.

Changing the position of the phenyl on the aminothiazole ring from C4 (**C12.2**: GAC IC_{50} > 200 μM, GDH inhibition 2%) to C5 (**C12.18**: GAC IC_{50} 12 μM, GDH inhibition 0%) considerably increased GAC inhibition while maintaining low GDH inhibition. Thus, C5 seems to be a better position for the phenyl group on ring B to inactivate GAC.

Directly combining the two better substituents found for rings A and C in **C12.30** (Table 6, GAC IC_{50} 17 μM, GDH inhibition 9%) afforded one of the best GAC inhibitors, which also showed low GDH inhibition, among the investigated series. Changing ring B from 2-aminothiazole to 5-amino-1,3,4-thiadiazole and increasing the distance between rings B and C by two atoms raised the activity towards GAC (**C12.33**: GAC IC_{50} 19 μM). Further increasing the distance between these two rings by adding an acetamide moiety decreased activity against GAC (**C12.34**: GAC IC_{50} 33 μM). Fig. 3 sums up all the observations found in our SAR study and additional studies and modifications to the **C12.30** structure could enhance its activity toward GAC [47–48].

Finally, we tested **C12.18**, **C12.30**, **C12.33,** and **C12.34** to evaluate their MDA-MB-231 cell/SKBR3 cell (Table 7) and GAC/GLS2 selectivity indices (Table 8). Our new batch of **C12** (from Chembridge) showed IC_{50} values of 28 (26–31) μM and 25 (23–27) μM in MDA-MB-231 and SKBR3 cells, respectively. We found that while **C12.18** had a similar IC_{50} against MDA-MB-231 and SKBR3 cell growth (18 μM for both), **C12.30** presented an IC_{50} value>200 μM in the SKBR3 cell line (Table 7). **C12.30** showed an IC_{50} value of 91 μM toward MDA-MB-231 growth, which supports that the 2-aminothiazole core can be used as a privileged scaffold for discovering selective GLS inhibitors. Compound **C12.30** also showed good selectivity when comparing its GAC (IC_{50} = 17 μM) and GLS2 (IC_{50} = 115 μM) inhibition (Table 8). As larger molecules seem to be more effective GLS inhibitors, further studies evaluating **C12.30**

Table 4
SAR evaluation of C12 ring A substituents on GAC and GDH inhibition.

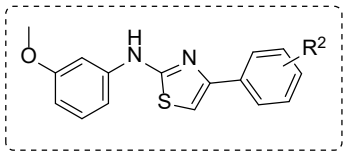

C12.1, C12.2, C12.4, C12.5, C12.19, C12.

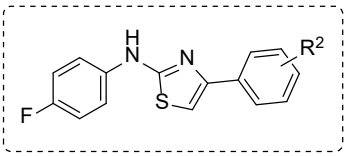

C12.20, C12.21, C12.22, C12.23, C12.24, C12.25, C12.26

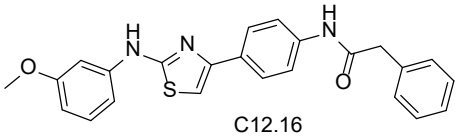

C12.16

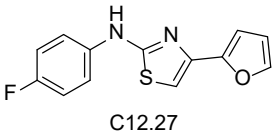

C12.27

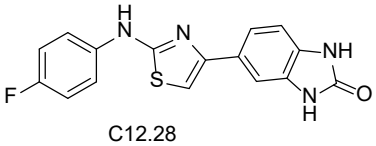

C12.28

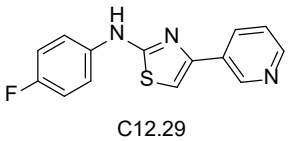

C12.29

Compound	R^1	IC_{50} [95% CI][a] (μM)	% of GDH Inhibition[b] (@ 200μM)
C12	**3-OMe**	**44** [35–52]	**81±9**
C12.3	3,5-bisCF_3	12 [9–14]	82 ± 6
C12.6	4-OMe	101 [94–107]	10 ± 10
C12.7	2-OMe	34 [27–41]	32 ± 5
C12.8	–	> 200	5 ± 7
C12.9	4-Cl	> 200	21 ± 10
C12.10	4-COOH	25 [20–31]	18 ± 11
C12.11	3,4,5-OMe	> 200	38 ± 1
C12.12	H	15 [13–17]	50 ± 16
C12.13	4-$COCH_3$	> 200	0
C12.14	4-CH_3	4 [3–5]	22 ± 3
C12.15	4-F	8 [6–9]	52 ± 20
C12.17	Phenylacetic	50 [32–68]	7 ± 6
CB-839	**–**	**0.0021 [0.0018–0.0025]**	**5±2**

[a] Values in μM, 95% Confidence Interval (CI).
[b] Values in percentage (%) compared to DMSO.

derivatives with additional larger substitutions on both rings could increase its activity even more.

As far as the toxicities of **C12.33** and **C12.34** in the MDA-MB-231 cell line are concerned, **C12.33** and **C12.34**, which are larger than **C12.30**, could fully inhibit MDA-MB-231 growth at the maximal dose (**Figure S2**) and showed IC_{50} values>200 μM in the SKBR3 cell line (Table 7). The IC_{50} values of propidium iodide- and caspase-3-activated staining, markers of cell necrosis and apoptosis, respectively, were 49.8 μM and 105.7 μM (**C12.33**) and 73.9 μM and 27.4 μM (**C12.34**) (**Figure S2**). Of note, **C12.33** and **C12.34** presented GLS2/GLS selectivity indices of 10.7 and 6, respectively, while the new batch of **C12** presented a selectivity index of 0.01 (Table 8). Based on these findings, **C12.33** and **C12.34** are the most selective compounds in the **C12** series.

To shed light on the molecular basis underlying the antiproliferative and GAC inhibition properties, we selected C12.34 as a representative inhibitor of the series and modelled its binding mode to the allosteric GAC binding site [1]. The modelling studies indicated that polar and hydrophobic interactions play central roles in inhibitor stabilization within GAC binding site (Fig. 4. For instance, favourable polar contacts between the carbonyl group of the amide substituent and the side chain of the Lys325C; the NH group of the amide substituent and the main chain carbonyl of Leu328B; and between the N3 and N4 atoms of the 1,3,4-thiadiazole core and the NH groups of Leu328B and Phe327B, respectively, were observed. Moreover, attractive hydrophobic interactions between the C12.34 substituents and the side chains of key binding site residues, including Phe327B, Phe327C, Tyr399B, Tyr399C, Leu326B, and Leu326C, were observed. These findings suggested the molecular determinants for the inhibition and are useful for the design of new analogues with enhanced activity.

Conclusions

The SAR study led to the discovery of new GAC inhibitors with improved activity and selectivity compared to C12. The most potent aminothiazole derivative (C12.30 Table 6) showed an IC_{50} value 2.6 times smaller than the hit C12 and enhanced selectivity towards the GLS, in comparison to GDH (improved from 80% to 9% inhibition). The selectivity index between glutaminase-dependent (MDA-MB-231) and non-dependant cells (SKBR3) was improved between 2 and 20 times (C12.30, C12.22 and C12.34, Table 7). Furthermore, there was a gain in selectivity between the isoforms GLS and GLS2, which was improved from 6 to 10 times (C12.30, C12.22 and C12.34, Table 8).

We observed that combining the 4-F and the phenylacetic modifications on ring A, the 1,3,4-thiadiazole moiety on ring B, and the 4-CN substituent on ring C seems to be the most promising combination of modifications to the structure of the hit **C12** toward improved GAC inhibition with low GDH activity. These modifications can be found in **C12.33** and **C12.34**, the most potent and selective inhibitors toward GAC and in MDA-MB-231 cells. **C12.30**, on the other hand, although less potent than **C12.33** and **C12.34**, was the best **C12** derivative containing

Table 5
SAR evaluation of C12 ring C substituents on GAC and GDH inhibition.

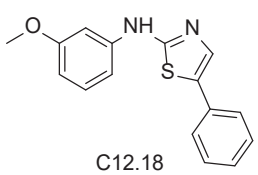

C12.18

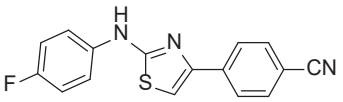

C12.30

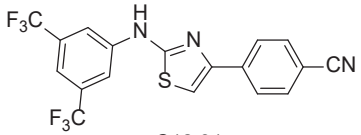

C12.31

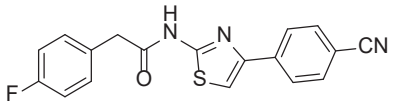

C12.32

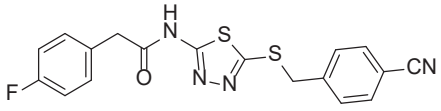

C12.33

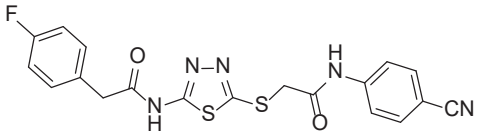

C12.34

Compound	R^2	IC_{50} [95% CI][a] (μM)	% of GDH Inhibition[b] (@ 200μM)
C12	**4-OH**	**44** [35–52]	**81±9**
C12.1	4-Ome	> 200	8 ± 9
C12.2	H	> 200	2 ± 8
C12.4	4-NO_2	99 [-57 – 254]	11 ± 9
C12.5	3,4-OH	29 [4–54]	81 ± 1
C12.16	4-NH Phenylacetic	36 [26–46]	14 ± 4
C12.19	4-CN	26 [22–31]	1 ± 6
C12.20	2,5-Ome	19 [12.2 – 25.4]	11 ± 3
C12.21	4-F	92 [-4 – 189]	12 ± 8
C12.22	4-CH_3	81 [22–139]	4 ± 5
C12.23	4-CF_3	38 [29–47]	9 ± 6
C12.24	4-Cl	65 [53–78]	11 ± 3
C12.25	3,5-CF_3	> 200	6 ± 2
C12.26	4-COOH	> 200	14 ± 4
C12.27	Furan-2-yl	132 [-35 – 299]	4 ± 5
C12.28	2-OH-benzimidazole-5-yl	73 [17–130]	13 ± 3
C12.29	Pyridin-3-yl	48 [34–62]	6 ± 5
CB-839	–	**0.0021 [0.0018 – 0.0025]**	**5±2**

[a] Values in μM 95% Confidence Interval (CI).
[b] Values in percentage (%) compared to DMSO.

an aminothiazole, presenting selectivity toward MDA-MB-231 cells and GAC similar to **C12.33** and **C12.34**. Taken together, these findings could be useful for the development of novel glutaminase inhibitors containing the aminothiazole scaffold, ultimately leading to new commercial drugs for cancer treatment targeting GLS1 enzyme inhibition, which is still pending.

Experimental section

GLS/GLS2-GDH and GDH activity assays

To determine the IC_{50} values of the compounds, serial dilutions of the compounds (in 1% DMSO) were mixed with 10 nM of purified enzyme in 50 mM Tris-acetate (pH 8.6), 0.2 mM EDTA, 2 mM NAD+, 0.6 U of GDH, 20 mM K_2HPO_4, and 7.5 mM glutamine. The GDH cross enzyme activity assay was performed under the same experimental conditions, removing the murine GAC enzyme (construct Δ1-127 [2]) from the assay, and replacing the glutamine substrate by the GDH-specific substrate, glutamate, also at a final concentration of 7.5 mM. For the GLS2 reaction, the reaction contained GLS2 at 5 nM and 3 U of GDH. Readings were performed on a PerkinElmer EnSpire 2300 multilabel plate reader at 340 nm. The percent activity was calculated based on the DMSO control reaction (100% activity). Adjustment of inhibitor dose–response curves was performed with the program GraphPad Prism v8.0 (GraphPad Software, USA) using the log (inhibitor) vs normalized response (variable slope) function. The inhibitor dose–response curves were adjusted with LL.4 model from drm r-package [53]. R-squared values obtained from drm [53] models using R2nls function from aomisc r-package. Standard deviations from fitted models were obtained using coeftest function from lmtest r-package. IC50 confidence interval were obtained using function ED from drm [53].

Cell culture

MDA-MB-231 (ATCC HTB-26) and SKBR3 (ATCC HTB-30) cells were obtained from the American Type Culture Collection (ATCC) and maintained in RPMI 1640 medium supplemented with 10% fetal bovine serum (FBS) at 37 °C under 5% CO2 in a humidified atmosphere. Cells used in in vitro assays were viable (90–100%), as evaluated with trypan blue staining.

Table 6
SAR evaluation of C12 ring B on GAC and GDH inhibition.

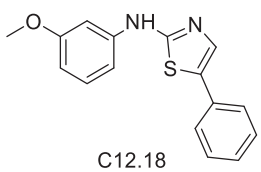

C12.18

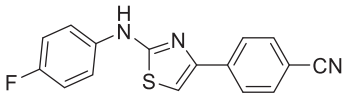

C12.30

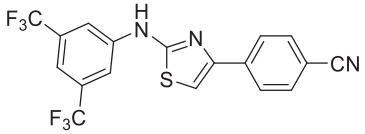

C12.31

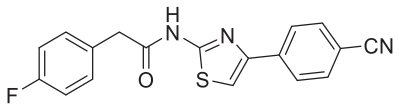

C12.32

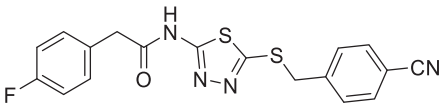

C12.33

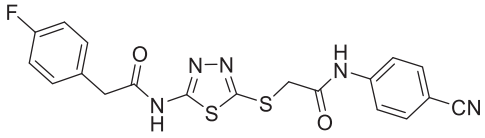

C12.34

Compound	IC_{50} [95% CI][a] (μM)	% of GDH Inhibition[b] (@ 200μM)
C12	**44** [35–52]	**81±9**
C12.18	12 [9–16]	0
C12.30	17 [11–23]	9 ± 3
C12.31	> 200	0
C12.32	63 [32–94]	22 ± 6
C12.33	19 [15–22]	10 ± 2
C12.34	33 [10–56]	13 ± 6
CB-839	**0.0021 [0.0018–0.0025]**	**5±2**

[a] Values in μM, 95% Confidence Interval (CI).
[b] Values in percentage (%) compared to DMSO.

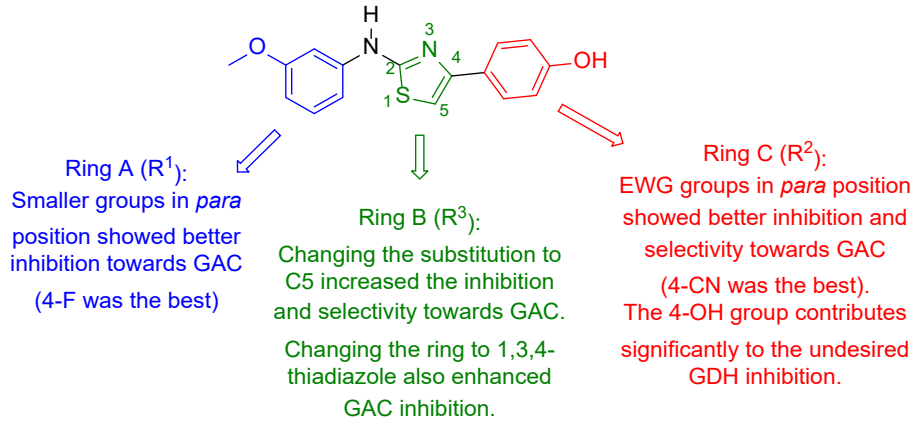

Fig. 3. Representation of the better substituents found for each **C12** ring.

Proliferation assay

Cells were seeded at a density of 2000 or 3000 cells/mm [2] in 96-well plates in complete medium. For the inhibition assays, the cells were incubated with complete medium containing vehicle (1% v/v of DMSO), CB-839 (Selleck Chemicals), C12 – C23 and C12 analogues 24 h after seeding and replenished 48 h hours later. Cells were fixed with 3.7% formaldehyde and stained with 0.4 μg/mL DAPI after 72 h of the first treatment. The stained nuclei were quantified using the fluorescence microscope and plate reader Operetta (PerkinElmer) and the software Columbus (PerkinElmer). Cell number was normalized by the final number of untreated cells (DMSO control, 100% cell growth) and the number of seeded cells (0% cell growth) to graphically show the dose that may lead to cell death (when the number of measured cells after treatment is smaller than the number of seeded cells). Adjustment of inhibitor dose–response curves was performed with the program GraphPad Prism (GraphPad Software, USA) using the log(inhibitor) vs response (variable slope) function.

Fluorescent cell assays

MDA-MB-231 cells were seeded at a density of 5000 cells/well in

Table 7
Selectivity of **C12**, **C12.18**, **C12.30**, **C12.33**, and **C12.34** in MDA-MB-231 *versus* SKBR3 cells.

Compounds	MDA-MB-231		SKBR3		Cell selectivity index IC_{50} SKBR3/IC_{50} MDA-MB-231)
	IC_{50} [95% CI][a] (μM)	R^2	IC_{50} [95% CI][a] (μM)	R^2	
C12	28 [26–31]	0.99	25 [23–27]	0.98	0.9
C12.18	18 [17–19]	0.99	18 [16–21]	0.96	1.0
C12.30	91 [57–194]	0.71	> 200	N/A	2.2
C12.33	36 [30–44]	0.94	> 200	N/A	5.5
C12.34	10 [7–12]	0.91	> 200	N/A	20.8

N/A indicates that this value could not be measured.
[a] Values in μM, 95% Confidence Interval (CI).

Table 8
Selectivity of **C12**, **C12.18**, **C12.30**, **C12.33** and **C12.34** against GAC *versus* GLS2.

Compounds	GAC		GLS2		Enzyme selectivity index (IC_{50} GLS2/ IC_{50} GLS)
	IC_{50} [95% CI][a] (μM)	R^2	IC_{50} [95% CI][a] (μM)	R^2	
C12	44 [35–52]	0.9	0.7 [0.7 – 0.8]	0.9	0.01
C12.18	12 [9–16]	0.8	8 [3–29]	0.8	0.7
C12.30	17 [11–23]	0.7	115 [38–6277]	0.7	6.6
C12.33	19 [15–22]	N/A	> 200	N/A	10.7
C12.34	33 [10–56]	N/A	> 200	N/A	6.0

N/A means that this value could not be measured.
[a] Values in μM 95% Confidence Interval (CI).

384-well plates in RPMI medium supplemented with 10% of heat-inactivated fetal bovine serum and 1% penicillin and G-streptomycin (Sigma-Aldrich). After seeding, the cells were incubated with the complete medium containing the vehicle (1% v/v of DMSO), serial dilutions of CB-839 (Selleck Chemicals), and C12 analogues (Chem- bridge) for 24 h. The culture medium was gently poured, and cells were then incubated with 1 μg/mL Propidium Iodide and 5 μg/mL Hoescht for 40 min in serum free medium, at 37 °C, 5% CO_2. Cells were evaluated with the fluorescence microscope and plate reader Operetta (PerkinElmer) and analysed with the software Columbus or Harmony (PerkinElmer). Cells were then fixed with 3.7% formaldehyde at room temperature for 20 min, washed twice in 1x PBS and permeabilized with 0.2% Triton X-100, 10% fetal bovine serum, in 1x PBS for 15 min at room temperature. Cells were incubated with primary antibody cleaved caspase-3 diluted 1:100 (RheaBiotech, # IM-0035) and 1% fetal bovine serum in 1x PBS at 37 °C for 3 h. Cells were washed twice in 1x PBS and were evaluated with microscope and plate reader Operetta (PerkinElmer) and analysed with the software Columbus or Harmony (PerkinElmer). Adjustment of inhibitor dose – response curves was performed with the program GraphPad Prism (GraphPad Software, USA) using the log(inhibitor) vs response (variable slope) function.

Dynamic light scattering

The mGAC enzyme was purified as previously described [25]. The assay was performed with either 500 mM or 150 mM NaCl. Filament assembly was induced by incubating freshly purified protein (in 150 mM NaCl buffer) with 20 mM K_2HPO_4. The protein was incubated for 24 h at 4 °C with each compound at 200 μM or 1% DMSO. Before measurement, all samples were microcentrifuged at 16.000 × g at 4 °C for 5 min. The sample was loaded into a quartz cuvette (ZMV1002, 1.25 mm light path, 105.231-QS, Hellma), and a SOP protocol was carried out on a Zetasizer μV (Malvern) after 120 s of primary equilibration at 10 °C. Measurements were performed in triplicate and analysed using Zetasizer software.

Thermal shift

The experiments were carried out on 96-well PCR plates and performed in a real-time thermal cycler (7500 Real-Time PCR System – Applied Biosystems). To each well was added 30 μL of a 10 μM GAC solution in 50 mM Tris buffer pH 8.6, 500 mM NaCl, 20 mM K_2HPO_4, plus 0.1% SYPRO® orange 5000-fold concentrated in DMSO (Invitrogen). Three hundred nanoliters of each compound was added to each well (1 mM stock and final equal to 10 μM). The temperature was scanned from 25 to 95 °C (1 °C/min) and fluorescence measurements performed. The fluorescence intensity was plotted as a function of temperature, generating a sigmoidal curve that can be described by two transition states (minimum and maximum fluorescence intensity, folded and denatured protein, respectively). The inflection point of the transition curve corresponds to the denaturation temperature of the protein (Tm) [54].

Molecular modelling

The 3D structure of C12.34 was constructed using standard geometric parameters of the molecular modeling ChemDraw and Chem3D software package (version 21). To generate the optimized conformation, the inhibitor structure was energetically minimized to a minimum RMS Gradient of 0.010 using the MM2 force field [3]. The C9.22 empirical atomic charges were computed by the Gasteiger-Hückel method [4]. Molecular docking of C9.22 was performed to GAC in complex with BPTES (PDB ID 4JKT) model using Surflex-Dock [5]. To investigate the binding mode of C12.34 to GAC, protein hydrogens and heavy atom movements were allowed to use default parameters. Histidine, glutamine, and asparagine residues within the binding site were manually checked for the possible flipped orientation, protonation, and tautomeric states. The binding cavity of the GAC was defined via the protomol generation that used the 3D coordinates of BPTES bound to GAC (Protomol parameters: proto_thresh 0.5 and -proto_bloat 5). The docking protocols were repeated 10 times. The Surflex-Dock scoring function and visual inspection were employed to select the representative conformation for inhibitor C12.34.

General procedure for the synthesis of the aminothiazoles

In a 5 mL microwave flask containing 3 mL of ethanol, the specific matchings of a thiourea (1 mmol) with a 2-bromoacetophenone (1 mmol) were added, The vial was then sealed and heated in a microwave reactor to 80 °C for 15 min. Then, the solvent was evaporated on a rotary evaporator and the residue obtained was purified by flash column chromatography using 7:3 hexane/acetone as eluent or by recrystallization in ethanol:water 8:2.

N-(3-methoxyphenyl)-4-(4-methoxyphenyl)thiazol-2-amine (C12.1) [55].

Prepared according to the general procedure for the synthesis of the aminothiazoles using *N*-(3-methoxyphenyl)thiourea and 2-bromo-4′-methoxyacetophenone. 87% yield, obtained as a white solid. M.p.: 158.4 – 160.7 °C (lit.: 159 – 161 °C). ^{1}H NMR (250 MHz, acetone-d_6, 2.05 ppm): δ 9.34 (s, 1H), 7.90 (d, J = 8.9 Hz, 2H), 7.65 (s, 1H), 7.17–7.26 (m, 2H), 6.99 (s, 1H), 6.97 (d, J = 8.9 Hz, 2H), 6.57 (dt, J = 7.1, 2.3 Hz, 1H), 3.82 (s, 3H), 3.83 (s, 3H). ^{13}C NMR (62.5 MHz, acetone-d_6, 29.84 ppm): δ 164.1, 161.4, 160.3, 151.8, 143.5, 130.5, 128.7, 128.0, 114.7, 110.3, 107.8, 103.9, 100.9, 55.5, 55.4. Melting point matches the literature.

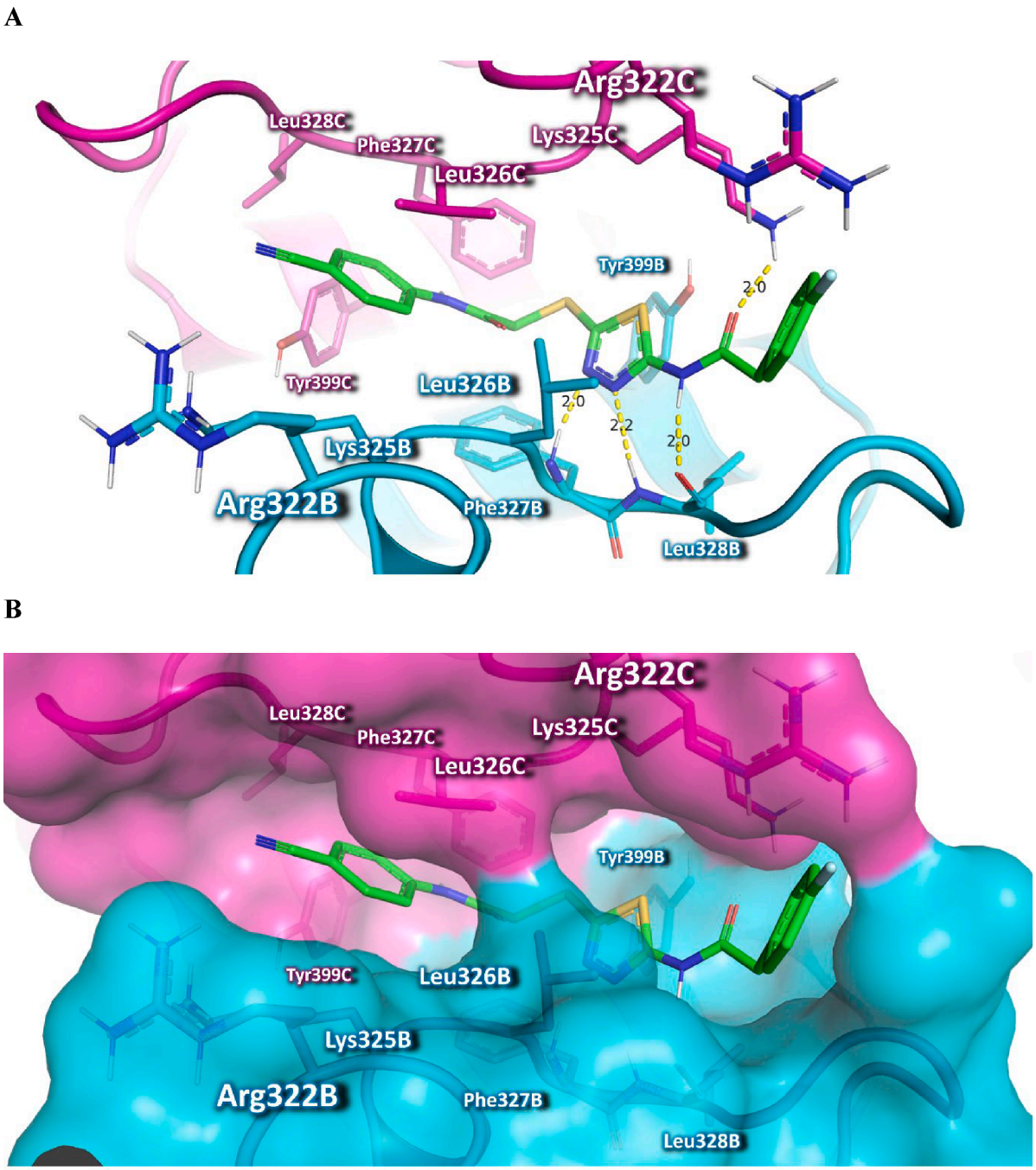

Fig. 4. Modelled binding mode of the GAC-C12.34 complex. The GAC structure (PDB ID 4JKT) is indicated as cartoon (**A**) and surface (**B**) models. Key residues involved in inhibitor (green) stabilization are indicated as stick models (subunits B and C are indicated as cyan and magenta, respectively). (For interpretation of the references to colour in this figure legend, the reader is referred to the web version of this article.)

NMR analysis in the literature was performed in DMSO-d_6 but also matches with our data. HPLC purity: 99%.

N-(3-methoxyphenyl)-4-phenylthiazol-2-amine (C12.2)

Prepared according to the general procedure for the synthesis of the aminothiazoles using *N*-(3-methoxyphenyl)thiourea and 2-bromoacetophenone. 86% yield, obtained as a white solid. M.p.: 211.1 – 212.8 °C. ^{1}H NMR (250 MHz, $CDCl_3$, 7.26 ppm): δ 11.71 (s, 1H), 7.79 (dd, $J = 7.9$, 1.8 Hz, 2H), 7.54–7.46 (m, 3H), 7.38 (t, $J = 8.0$ Hz, 1H), 6.97 (d, $J = 7.9$ Hz, 1H), 6.85–6.90 (m, 2H), 6.66 (s, 1H), 3.84 (s, 3H). ^{13}C NMR (62.5 MHz, $CDCl_3$, 77.16 ppm): δ 168.1, 161.1, 141.1, 137.7, 131.1, 130.8, 129.7, 127.1, 126.0, 113.4, 112.9, 107.0, 98.3, 55.7. HRMS (ESI +): *m/z* calculated for $C_{16}H_{15}N_2OS^+$ [M + H^+] 283.08996, found 283.08969. HPLC purity: 99%.

4-(2-((3,5-bis(trifluoromethyl)phenyl)amino)thiazol-4-yl)phenol (C12.3)

Prepared according to the general procedure for the synthesis of the aminothiazoles using 1-(3,5-bis(trifluoromethyl)phenyl)thiourea and 2-bromo-4′-methoxyacetophenone. 92% yield, obtained as a light greenish solid. M.p.: 247.3 – 249.0 °C. ^{1}H NMR (250 MHz, DMSO-d_6, 2.50 ppm): δ 11.08 (s, 1H), 9.48 (s, 1H), 8.47 (s, 2H), 7.71 (d, $J = 8.3$ Hz, 2H), 7.56 (s, 1H), 7.22 (s, 1H), 6.81 (d, $J = 8.3$ Hz, 2H). ^{13}C NMR (62.5 MHz, DMSO-d_6, 39.52 ppm): δ 142.7, 130.9 (q, $J_{C\text{-}F} = 32.3$ Hz), 126.9, 125.5, 123.4 (q, $J_{C\text{-}F} = 271.2$ Hz), 116.2, 115.4, 113.1, 101.7. ^{19}F NMR (235 MHz, DMSO-d_6): δ −61.79. HRMS (ESI +): *m/z* calculated for

$C_{17}H_{11}F_6N_2OS^+$ [M + H^+] 405.0491, found 405.0499. HPLC purity: 97%.

N-(3-methoxyphenyl)-4-(4-nitrophenyl)thiazol-2-amine (C12.4)

Prepared according to the general procedure for the synthesis of the aminothiazoles using *N*-(3-methoxyphenyl)thiourea and 2-bromo-4′-nitroacetophenone. 96% yield, obtained as a yellow solid. M.p.: 172.5 – 147 °C. ^{1}H NMR (250 MHz, DMSO-d_6, 2.50 ppm): δ 10.43 (s, 1H), 8.29 (d, J = 8.9 Hz, 2H), 8.14 (d, J = 8.9 Hz, 2H), 7.72 (s, 1H), 7.51 (t, J = 2.0 Hz, 1H), 7.27–7.16 (m, 2H), 6.56 (dt, J = 7.1, 2.3 Hz, 1H), 3.78 (s, 3H). ^{13}C NMR (62.5 MHz, DMSO-d_6, 39.52 ppm): δ 163.4, 159.8, 147.9, 146.2, 142.0, 140.4, 129.8, 126.4, 124.1, 109.4, 108.0, 107.0, 102.7, 54.9. HRMS (ESI +): *m/z* calculated for $C_{16}H_{14}N_3O_3S^+$ [M + H^+] 328.07504, found 328.07458. HPLC purity: 98%.

4-(2-((3-methoxyphenyl)amino)thiazol-4-yl)benzene-1,2-diol (C12.5)

Prepared according to the general procedure for the synthesis of the aminothiazoles using *N*-(3-methoxyphenyl)thiourea and 2-bromo-3′,4′-dihydroxyacetophenone. 84% yield, obtained as a greyish solid. M.p.: 204.1 – 205.4 °C. ^{1}H NMR (250 MHz, DMSO-d_6, 2.50 ppm): δ 10.47 (s, 1H), 9.45 (s, 2H), 7.47 (t, J = 1.9 Hz, 1H), 7.29 (d, J = 1.9 Hz, 1H), 7.22 (d, J = 8.1 Hz, 1H), 7.17–7.14 (m, 2H), 6.98 (s, 1H), 6.79 (d, J = 8.1 Hz, 1H), 6.57 (dt, J = 7.1, 2.3 Hz, 1H), 3.77 (s, 3H). ^{13}C NMR (62.5 MHz, DMSO-d_6, 39.52 ppm): δ 163.2, 159.9, 149.3, 145.5, 145.2, 142.1, 129.8, 125.7, 117.2, 115.8, 113.5, 109.7, 107.1, 103.1, 100.0, 54.9. HRMS (ESI +): *m/z* calculated for $C_{16}H_{15}N_2O_3S^+$ [M + H^+] 315.07979, found 315.07924. HPLC purity: 95%.

4-(2-((4-methoxyphenyl)amino)thiazol-4-yl)phenol (C12.6)

Prepared according to the general procedure for the synthesis of the aminothiazoles using *N*-(4-methoxyphenyl)thiourea and 2-bromo-4′-hydroxyacetophenone. 88% yield, obtained as a grey solid. M.p.: 210.1 – 212 °C. ^{1}H NMR (250 MHz, acetone-d_6, 2.05 ppm): δ 9.03 (s, 1H), 8.54 (s, 1H), 7.80 (d, J = 8.9 Hz, 2H), 7.68 (d, J = 8.9 Hz, 2H), 6.95–6.85 (m, 4H), 6.85 (s, 1H), 3.78 (s, 3H). ^{13}C NMR (62.5 MHz, acetone-d_6, 29.84 ppm): δ 165.1, 158.0, 155.8, 152.1, 135.8, 128.1, 127.9, 120.1, 116.0, 115.0, 99.5, 55.6. HRMS (ESI +): *m/z* calculated for $C_{16}H_{15}N_2O_2S^+$ [M + H^+] 299.08487, found 299.08448. HPLC purity: 98%.

4-(2-((2-methoxyphenyl)amino)thiazol-4-yl)phenol (C12.7)

Prepared according to the general procedure for the synthesis of the aminothiazoles using *N*-(2-methoxyphenyl)thiourea and 2-bromo-4′-hydroxyacetophenone. 85% yield, obtained as a white solid. M.p.: 237.5 – 238.7 °C. ^{1}H NMR (250 MHz, DMSO-d_6, 2.50 ppm): δ 9.83 (s, 1H), 8.33 (s, 1H), 8.25 (d, J = 7.4 Hz, 1H), 7.08–6.96 (m, 3H), 7.66 (d, J = 8.5 Hz, 2H), 7.03 (s, 1H), 6.82 (d, J = 8.5 Hz, 2H), 3.86 (s, 3H). ^{13}C NMR (62.5 MHz, DMSO-d_6, 39.52 ppm): δ 164.7, 157.4, 149.0, 147.5, 129.2, 127.2, 124.4, 123.5, 120.7, 119.5, 115.4, 111.3, 100.6, 55.7. HRMS (ESI +): *m/z* calculated for $C_{16}H_{15}N_2O_2S^+$ [M + H^+] 299.08487, found 299.08444. HPLC purity: 97%.

4-(2-aminothiazol-4-yl)phenol (C12.8) [56–57].

Prepared according to the general procedure for the synthesis of the aminothiazoles using thiourea and 2-bromo-4′-hydroxyacetophenone. 99% yield, obtained as a white solid. M.p: 233.7–234.4 °C (lit.: 234.4–234.6 °C) [57]. ^{1}H NMR (250 MHz, acetone-d_6, 2.05 ppm): δ 8.39 (s, 1H), 7.69 (d, J = 8.7 Hz, 2H), 6.81 (d, J = 8.7 Hz, 2H), 6.69 (s, 1H), 6.33 (s, 2H). ^{13}C NMR (62.5 MHz, acetone-d_6, 29.84 ppm): δ 168.7, 157.7, 151.8, 128.1, 128.0, 115.9, 99.7. Melting point matches the literature. NMR analysis in the literature was performed in DMSO-d_6 but also matches with our data. HPLC purity: 97%.

4-(2-((4-chlorophenyl)amino)thiazol-4-yl)phenol (C12.9) [58].

Prepared according to the general procedure for the synthesis of the aminothiazoles using 1-(4-chlorophenyl)thiourea and 2-bromo-4′-hydroxyacetophenone. 86% yield, obtained as a greyish solid. M.p.: 187.5 – 188.3 °C (lit.: 188.7 °C) ^{1}H NMR (250 MHz, DMSO-d_6, 2.50 ppm): δ 10.43 (s, 1H) 7.74 (t, J = 9.1 Hz, 4H), 7.37 (d, J = 8.6 Hz, 2H), 7.08 (s, 1H), 6.81 (d, J = 8.6 Hz, 2H). ^{13}C NMR (62.5 MHz, DMSO-d_6, 39.52 ppm): δ 162.7, 157.2, 150.0, 140.1, 128.8, 127.1, 125.6, 124.5, 118.4, 115.3, 100.3. Melting point and NMR data agree with the literature. HPLC purity: 95%.

4-((4-(4-hydroxyphenyl)thiazol-2-yl)amino)benzoic acid (C12.10)

Prepared according to the general procedure for the synthesis of the aminothiazoles using 4-thioureidobenzoic acid and 2-bromo-4′-hydroxyacetophenone. 87% yield, obtained as brownish solid. M.p.: 253.2 – 256.6 °C. ^{1}H NMR (250 MHz, DMSO-d_6, 2.50 ppm): δ 10.62 (s, 1H), 9.57 (s, 1H), 7.93 (d, 8.8 Hz, 2H), 7.80 (d, J = 8.8 Hz, 2H), 7.76 (d, J = 8.5 Hz, 2H), 7.15 (s, 1H), 6.82 (d, J = 8.5 Hz, 2H). ^{13}C NMR (62.5 MHz, DMSO-d_6, 39.52 ppm): δ 167.0, 162.0, 157.2, 150.5, 145.0, 130.8, 127.1, 125.7, 122.6, 115.8, 115.4, 101.0. HRMS (ESI +): *m/z* calculated for $C_{16}H_{13}N_2O_3S^+$ [M + H^+] 313.06414, found 313.06355. HPLC purity: 91%.

4-(2-((3,4,5-trimethoxyphenyl)amino)thiazol-4-yl)phenol (C12.11)

Prepared according to the general procedure for the synthesis of the aminothiazoles using 3,4,5-trimethoxyphenylthiourea and 2-bromo-4′-hydroxyacetophenone. 84% yield, obtained as white solid. M.P.: 213.1 – 215.5 °C. ^{1}H NMR (250 MHz, CD_3OD, 3.31 ppm): δ 7.93 (s, 1H), 7.53 (d, J = 8.6 Hz, 2H), 6.91 (d, J = 8.6 Hz, 2H), 6.84 (s, 2H), 3.87 (s, 6H), 3.79 (s, 3H). ^{13}C NMR (62.5 MHz, CD_3OD, 49.15 ppm): δ 171.5, 160.8, 155.8, 142.6, 138.8, 135.0, 129.2, 121.0, 117.1, 102.2, 79.6, 61.3, 57.0. HRMS (ESI +): *m/z* calculated for $C_{18}H_{19}N_2O_4S^+$ [M + H^+] 359.1060, found 359.1049. HPLC purity: 96%.

4-(2-(phenylamino)thiazol-4-yl)phenol (C12.12) [56].

Prepared according to the general procedure for the synthesis of the aminothiazoles using phenylthiourea and 2-bromo-4′-hydroxyacetophenone. 98% yield, obtained as a white solid. M.p.: 163.9 – 165.3 °C. ^{1}H NMR (250 MHz, acetone-d_6, 2.05 ppm): δ 9.27 (s, 1H), 8.47 (s, 1H), 7.80 (t, J = 8.3 Hz, 4H), 7.34 (t, J = 7.5 Hz, 2H), 6.98 (t, J = 7.5 Hz, 1H), 6.93 (s, 1H), 6.89 (d, J = 8.5 Hz, 2H). ^{13}C NMR (62.5 MHz, acetone-d_6, 29.84 ppm): δ 164.1, 158.0, 152.1, 142.4, 129.8, 128.2, 127.8, 122.3, 118.0, 116.1, 100.2. NMR analysis in the literature was performed in DMSO-d_6 but also matches with our data. HPLC purity: 98%.

1-(4-((4-(4-hydroxyphenyl)thiazol-2-yl)amino)phenyl)ethanone (C12.13)

Prepared according to the general procedure for the synthesis of the aminothiazoles using 1-(4-acetylphenyl)thiourea and 2-bromo-4′-hydroxyacetophenone. 85% yield, obtained as a yellow solid. M.p.: 234.2 – 235.4 °C. ^{1}H NMR (250 MHz, acetone-d_6, 2.05 ppm): δ 9.69 (s, 1H), 8.50 (s, 1H), 8.01 (d, J = 8.8 Hz, 2H), 7.92 (d, J = 8.8 Hz, 2H), 7.85 (d, J = 8.5 Hz, 2H), 7.06 (s, 1H), 6.90 (d, J = 8.5 Hz, 2H), 2.54 (s, 3H). ^{13}C NMR (62.5 MHz, acetone-d_6, 29.84 ppm): δ 196.2, 163.1, 158.2, 152.3, 146.3, 131.4, 130.7, 128.2, 127.6, 116.9, 116.2, 101.6, 26.3. HRMS (ESI +): *m/z* calculated for $C_{17}H_{15}N_2O_2S^+$ [M + H^+] 311.0849, found 311.0846. HPLC purity: 91%.

4-(2-(p-tolylamino)thiazol-4-yl)phenol (C12.14) [59].

Prepared according to the general procedure for the synthesis of the aminothiazoles using 4-methylphenylthiourea and 2-bromo-4′-hydroxyacetophenone. 91% yield, obtained as a White solid. M.p.: 198.3 – 199.5 °C. ^{1}H NMR (250 MHz, acetone-d_6, 2.05 ppm): δ 9.14 (s, 1H), 8.48 (s, 1H), 7.81 (d, J = 8.4 Hz, 2H), 7.66 (d, J = 8.2 Hz, 2H), 7.15 (d, J = 8.2 Hz, 2H), 6.89 (s, 1H), 6.88 (d, J = 8.4 Hz, 2H), 2.28 (s, 3H). ^{13}C NMR (62.5 MHz, acetone-d_6, 29.84 ppm): δ 164.5, 158.0, 152.1, 140.0, 131.6, 130.2, 128.1, 127.9, 118.3, 116.1, 99.9, 20.7. NMR analysis in the literature was performed in MeOD-d_4 but also matches with our data. HPLC purity: 99%.

4-(2-((4-fluorophenyl)amino)thiazol-4-yl)phenol (C12.15) [58].

Prepared according to the general procedure for the synthesis of the aminothiazoles using 1-(4-fluorophenyl)thiourea and 2-bromo-4′-hydroxyacetophenone. 89% yield, obtained as a greyish solid. M.p.: 174.4 – 175.7 °C (lit.: 176 °C). ^{1}H NMR (250 MHz, acetone-d_6, 2.05 ppm): δ 9.28 (s, 1H), 8.48 (s, 1H), 7.86–7.79 (m, 4H), 7.12 (t, J = 8.9 Hz, 2H), 6.93 (s, 1H), 6.88 (d, J = 8.6 Hz, 2H). ^{13}C NMR (62.5 MHz, acetone-d_6, 29.84 ppm): δ 164.2, 158.5 (d, $J_{C\text{-}F}$ = 236.6 Hz), 158.12, 152.1, 138.9 (d, $J_{C\text{-}F}$ = 2.1 Hz), 128.2, 127.8, 119.6 (d, $J_{C\text{-}F}$ = 7.5 Hz), 116.2 (d, $J_{C\text{-}F}$ = 22.3 Hz), 116.1, 100.2. ^{19}F NMR (235 MHz, acetone-d_6): δ −123.5. Melting point matches the literature. NMR analysis in the

literature was performed in DMSO-d_6 but also matches with our data. HPLC purity: 98% [58].

4-(2-((3-methoxyphenyl)amino)thiazol-4-yl)benzonitrile (C12.19)

Prepared according to the general procedure for the synthesis of the aminothiazoles using *N*-(3-methoxyphenyl)thiourea and 4-(2-bromoacetyl)benzonitrile. 84% yield, slightly yellowish solid. M.p.: 151.1 – 153.2 °C. ^{1}H NMR (250 MHz, $CDCl_3$, 7.26 ppm): δ 7.94 (d, J = 8.4 Hz, 2H), 7.67 (d, J = 8.4 Hz, 2H), 7.23–7.30 (m, 2H), 7.10 (t, J = 2.2 Hz, 1H), 6.98–6.94 (m, 2H), 6.65 (dd, J = 8.3, 1.9 Hz, 1H), 3.83 (s, 3H). ^{13}C NMR (62.5 MHz, $CDCl_3$, 77.16 ppm): δ 164.8, 160.6, 149.3, 141.3, 138.5, 132.6, 130.3, 126.5, 119.1, 111.0, 110.7, 108.7, 105.0, 104.4, 55.4. HRMS (ESI +): *m/z* calculated for $C_{17}H_{14}N_3OS^+$ [M + H$^+$] 308.0852, found 308.0837. HPLC purity: 97%.

4-(2,5-dimethoxyphenyl)-N-(4-fluorophenyl)thiazol-2-amine (C12.20)

Prepared according to the general procedure for the synthesis of the aminothiazoles using 1-(4-fluorophenyl)thiourea and 2-bromo-1-(2,5-dimethoxyphenyl)ethanone. 93% yield, obtained as a brownish oil. ^{1}H NMR (250 MHz, $CDCl_3$, 7.26 ppm): δ 7.71 (d, J = 3.0 Hz, 1H), 7.37–7.31 (m, 2H), 7.31 (s, 1H), 7.02 (t, $J_{H\text{-}H\text{-}F}$ = 8.4 Hz, 2H), 6.90 (d, J = 8.9 Hz, 1H), 6.81 (dd, J = 8.8, 3.0 Hz, 1H), 3.89 (s, 3H), 3.80 (s, 3H). ^{13}C NMR (62.5 MHz, $CDCl_3$, 77.16 ppm): δ 163.7, 158.9 (d, $J_{C\text{-}F}$ = 240.8 Hz), 153.7, 151.4, 146.9, 136.8 (d, $J_{C\text{-}F}$ = 2.6 Hz), 123.8, 102.6 (d, $J_{C\text{-}F}$ = 7.9 Hz), 116.1 (d, $J_{C\text{-}F}$ = 22.5 Hz), 115.0, 114.1, 112.5, 106.9, 56.1, 55.9. ^{19}F NMR (235 MHz, $CDCl_3$): δ −119.6. HRMS (ESI +): *m/z* calculated for $C_{17}H_{16}FN_2O_2S^+$ [M + H$^+$] 331.0911, found 331.0910. HPLC purity: 91%.

N,4-bis(4-fluorophenyl)thiazol-2-amine (C12.21) [60,61].

Prepared according to the general procedure for the synthesis of the aminothiazoles using 1-(4-fluorophenyl)thiourea and 2-bromo-1-(4-fluorophenyl)ethanone. 97% yield, obtained as a slightly greenish solid. M.p.: 125.9 – 127.4 °C (lit.: 127 °C). ^{1}H NMR (250 MHz, $CDCl_3$, 7.26 ppm): δ 7.79 (dd, J = 8.8 Hz, $J_{H\text{-}F}$ = 5.4 Hz, 2H), 7.74 (s, 1H), 7.33 (dd, J = 9.2 Hz, $J_{H\text{-}F}$ = 4.6 Hz, 2H), 7.09–6.99 (m, 4H), 6.71 (s, 1H). ^{13}C NMR (62.5 MHz, $CDCl_3$, 77.16 ppm): δ 165.7, 162.8 (d, $J_{C\text{-}F}$ = 225.5 Hz), 158.9 (d, $J_{C\text{-}F}$ = 221.3 Hz), 150.6, 136.5 (d, $J_{C\text{-}F}$ = 2.6 Hz), 130.9 (d, $J_{C\text{-}F}$ = 3.2 Hz), 127.9 (d, $J_{C\text{-}F}$ = 8.0 Hz), 121.0 (d, $J_{C\text{-}F}$ = 7.9 Hz), 116.3 (d, $J_{C\text{-}F}$ = 22.5 Hz), 115.6 (d, $J_{C\text{-}F}$ = 21.5 Hz), 101.3. ^{19}F NMR (235 MHz, $CDCl_3$) δ −113.9, −119.0. Melting point and NMR data agree with the literature. HPLC purity: 99%.

N-(4-fluorophenyl)-4-(p-tolyl)thiazol-2-amine (C12.22) [62].

Prepared according to the general procedure for the synthesis of the aminothiazoles using 1-(4-fluorophenyl)thiourea and 2-bromo-1-(p-tolyl)ethanone. 92% yield, obtained as a white solid. M.p.: 165.4 – 166.7 °C. ^{1}H NMR (250 MHz, $CDCl_3$, 7.26 ppm): δ 8.02 (s, 1H), 7.70 (d, J = 8.0 Hz, 2H), 7.30 (dd, J = 8.9 Hz, $J_{H\text{-}F}$ = 4.6 Hz, 2H), 7.17 (d, J = 8.0 Hz, 2H), 7.00 (t, $J_{H\text{-}H\text{-}F}$ = 8.3 Hz, 2H), 6.72 (s, 1H), 2.36 (s, 3H). ^{13}C NMR (62.5 MHz, $CDCl_3$, 77.16 ppm): δ 165.7, 158.9 (d, $J_{C\text{-}F}$ = 241.0 Hz), 151.6, 137.8, 136.7 (d, $J_{C\text{-}F}$ = 2.6 Hz), 131.9, 129.4, 126.1, 120.9 (d, $J_{C\text{-}F}$ = 7.9 Hz), 116.1 (d, $J_{C\text{-}F}$ = 22.5 Hz), 100.9, 21.3. ^{19}F NMR (235 MHz, $CDCl_3$): δ −120.1. NMR data matches literature. HPLC purity: 96%.

N-(4-fluorophenyl)-4-(4-(trifluoromethyl)phenyl)thiazol-2-amine (C12.23)

Prepared according to the general procedure for the synthesis of the aminothiazoles using 1-(4-fluorophenyl)thiourea and 2-bromo-1-(4-(trifluoromethyl)phenyl)ethanone. 88% yield, obtained as a white solid. M.p.: 181.7 – 183.1 °C. ^{1}H NMR (400 MHz, $CDCl_3$, 7.26 ppm): δ 8.10 (s, 1H), 7.87 (d, J = 8.1 Hz, 2H), 7.57 (d, J = 8.1 Hz, 2H), 7.31 (dd, J = 8.5 Hz, $J_{H\text{-}F}$ = 4.4 Hz, 2H), 6.99 (t, $J_{H\text{-}H\text{-}F}$ = 8.5 Hz, 2H), 6.83 (s, 1H). ^{13}C NMR (100 MHz, $CDCl_3$, 77.16 ppm): δ 166.6, 159.4 (d, $J_{C\text{-}F}$ = 242.3 Hz), 149.2, 137.2, 136.1 (d, $J_{C\text{-}F}$ = 2.6 Hz), 129.9 (q, $J_{C\text{-}F}$ = 32.3 Hz), 126.4, 125.7 (d, $J_{C\text{-}F}$ = 3.7 Hz), 124.2 (q, $J_{C\text{-}F}$ = 270.5 Hz), 121.5 (d, $J_{C\text{-}F}$ = 7.8 Hz), 116.3 (d, $J_{C\text{-}F}$ = 22.5 Hz), 103.3. ^{19}F NMR (235 MHz, $CDCl_3$): δ −118.5 (1F), −62.4 (3F). HRMS (ESI +): *m/z* calculated for $C_{16}H_{11}F_4N_2S^+$ [M + H$^+$] 339.0574, found 339.0558. HPLC purity: 97%.

4-(4-chlorophenyl)-N-(4-fluorophenyl)thiazol-2-amine (C12.24) [63,64].

Prepared according to the general procedure for the synthesis of the aminothiazoles using 1-(4-fluorophenyl)thiourea and 2-bromo-1-(4-chlorophenyl)ethanone. 86% yield, obtained as a white solid. M.p.: 167.2 – 168.6 °C (lit.: 168–169 °C). ^{1}H NMR (250 MHz, $CDCl_3$, 7.26 ppm): δ 7.87 (s, 1H), 7.73 (d, J = 8.5 Hz, 2H), 7.34–7.29 (m, 4H), 7.02 (t, $J_{H\text{-}H\text{-}F}$ = 8.5 Hz, 2H), 6.75 (s, 1H). ^{13}C NMR (62.5 MHz, $CDCl_3$, 77.16 ppm): δ 151.3, 144.5 (d, $J_{C\text{-}F}$ = 241.5 Hz), 135.7, 121.8 (d, $J_{C\text{-}F}$ = 2.6 Hz), 119.1, 118.4, 114.2, 112.8, 106.4 (d, $J_{C\text{-}F}$ = 7.8 Hz), 101.6 (d, $J_{C\text{-}F}$ = 22.5 Hz), 87.45. ^{19}F NMR (235 MHz, $CDCl_3$): δ −118.8. Melting point and NMR data agree with the literature. HPLC purity: 97%.

4-(3,5-bis(trifluoromethyl)phenyl)-N-(4-fluorophenyl)thiazol-2-amine (C12.25)

Prepared according to the general procedure for the synthesis of the aminothiazoles using 1-(4-fluorophenyl)thiourea and 1-(3,5-bis(trifluoromethyl)phenyl)-2-bromoethanone. 85% yield, obtained as a greyish solid. M.p.: 253.1 – 254.9 °C. ^{1}H NMR (250 MHz, DMSO-d_6, 2.50 ppm): δ 10.46 (s, 1H), 8.50 (s, 2H), 7.99 (s, 1H), 7.88 (s, 1H), 7.31 (dd, J = 9.1 Hz, $J_{H\text{-}F}$ = 4.8 Hz, 2H), 7.19 (t, $J_{H\text{-}H\text{-}F}$ = 8.9 Hz, 2H). ^{13}C NMR (62.5 MHz, DMSO-d_6, 39.52 ppm): δ 163.9, 157.1 (d, $J_{C\text{-}F}$ = 234.4 Hz), 146.7, 137.3 (d, $J_{C\text{-}F}$ = 1.9 Hz), 136.7, 130.8 (q, $J_{C\text{-}F}$ = 32.4 Hz), 125.7, 123.4 (q, $J_{C\text{-}F}$ = 271.4 Hz), 120.6 (q, $J_{C\text{-}F}$ = 3.5 Hz), 118.7 (d, $J_{C\text{-}F}$ = 7.7 Hz), 115.6 (d, $J_{C\text{-}F}$ = 22.2 Hz), 107.1. ^{19}F NMR (235 MHz, DMSO-d_6): δ −61.3 (6F), −121.3 (1F). HRMS (ESI +): *m/z* calculated for $C_{17}H_{10}F_7N_2S^+$ [M + H$^+$] 407.0447, found 407.0458. HPLC purity: 98%.

4-(2-((4-fluorophenyl)amino)thiazol-4-yl)benzoic acid (C12.26)

Prepared according to the general procedure for the synthesis of the aminothiazoles using 1-(4-fluorophenyl)thiourea and 4-(2-bromoacetyl) benzoic acid. 85% yield, obtained as a white solid. M.p.: 268.2 – 271.1 °C. ^{1}H NMR (250 MHz, DMSO-d_6, 2.50 ppm): δ 10.40 (s, 1H), 9.01 (s, 1H), 8.04–7.96 (m, 4H), 7.76 (dd, J = 8.8 Hz, $J_{H\text{-}F}$ = 4.7 Hz, 2H), 7.52 (s, 1H), 7.19 (t, $J_{H\text{-}H\text{-}F}$ = 8.8 Hz, 2H). ^{13}C NMR (62.5 MHz, DMSO-d_6, 39.52 ppm): δ 167.1, 163.4, 156.4 (d, $J_{C\text{-}F}$ = 236.0 Hz), 148.9, 138.3, 137.6 (d, $J_{C\text{-}F}$ = 2.1 Hz), 129.8, 129.5, 125.6, 118.5 (d, $J_{C\text{-}F}$ = 7.4 Hz), 115.6 (d, $J_{C\text{-}F}$ = 22.0 Hz), 105.6. ^{19}F NMR (235 MHz, DMSO-d_6): δ −121.8. HRMS (ESI +): *m/z* calculated for $C_{16}H_{12}FN_2O_2S^+$ [M + H$^+$] 315.0598, found 315.0600. HPLC purity: 91%.

N-(4-fluorophenyl)-4-(furan-2-yl)thiazol-2-amine (C12.27)

Prepared according to the general procedure for the synthesis of the aminothiazoles using 1-(4-fluorophenyl)thiourea and 2-bromo-1-(furan-2-yl)ethanone. 99% yield, obtained as a brown solid. M.p.: 132.4 – 133.7 °C. ^{1}H NMR (250 MHz, $CDCl_3$, 7.26 ppm): δ 8.17 (s, 1H), 7.36–7.35 (m, 1H), 7.31 (dd, J = 9.0 Hz, $J_{H\text{-}F}$ = 4.5 Hz, 2H), 7.03 (t, $J_{H\text{-}H\text{-}F}$ = 8.7 Hz, 2H), 6.74 (s, 1H), 6.64 (d, J = 3.2 Hz, 1H), 6.41 (dd, J = 3.2 Hz, 1.8 Hz, 1H). ^{13}C NMR (62.5 MHz, $CDCl_3$, 77.16 ppm): δ 166.6, 159.2 (d, $J_{C\text{-}F}$ = 241.5 Hz), 150.1, 142.9, 142.1, 136.5 (d, $J_{C\text{-}F}$ = 2.3 Hz), 121.5 (d, $J_{C\text{-}F}$ = 8.0 Hz), 116.3 (d, $J_{C\text{-}F}$ = 22.5 Hz), 111.4, 106.9, 101.1. ^{19}F NMR (235 MHz, $CDCl_3$): δ −120.1. HRMS (ESI +): *m/z* calculated for $C_{13}H_{10}FN_2OS^+$ [M + H$^+$] 261.0492, found 261.0477. HPLC purity: 98%.

5-(2-((4-fluorophenyl)amino)thiazol-4-yl)-1H-benzo[d]imidazol-2(3H)-one (C12.28)

Prepared according to the general procedure for the synthesis of the aminothiazoles using 1-(4-fluorophenyl)thiourea and 5-(2-chloroacetyl)-1H-benzo[*d*]imidazol-2(3H)-one. 84% yield, obtained as a yellowish solid. M.p.: 358.1 – 361.6 °C. ^{1}H NMR (250 MHz, DMSO-d_6, 2.50 ppm): δ 10.65 (s, 2H), 10.23 (s, 1H), 7.72 (dd, J = 8.7 Hz, $J_{H\text{-}F}$ = 4.6 Hz, 2H), 7.53 (d, J = 8.3 Hz, 1H), 7.44 (s, 1H), 7.17 (t, $J_{H\text{-}H\text{-}F}$ = 8.4 Hz, 2H), 7.13 (s, 1H), 6.95 (d, J = 8.0 Hz, 1H). ^{13}C NMR (62.5 MHz, DMSO-d_6, 39.52 ppm): δ 163.0, 156.7 (d, $J_{C\text{-}F}$ = 236.1 Hz), 155.5, 150.6, 137.8 (d, $J_{C\text{-}F}$ = 1.7 Hz), 130.0, 129.4, 127.6, 118.6, 118.3 (d, $J_{C\text{-}F}$ = 7.0 Hz), 115.5 (d, $J_{C\text{-}F}$ = 21.6 Hz), 108.5, 106.0, 100.5. ^{19}F NMR (235 MHz, DMSO-d_6): δ −122.0. HRMS (ESI +): *m/z* calculated for $C_{16}H_{12}FN_4OS^+$ [M + H$^+$] 327.0710, found 327.0704. HPLC purity: insoluble in HPLC column compatible solvents.

N-(3-methoxyphenyl)-4-(pyridin-3-yl)thiazol-2-amine (C12.29)

Prepared according to the general procedure for the synthesis of the aminothiazoles using *N*-(3-methoxyphenyl)thiourea and 2-bromo-1-

(pyridin-3-yl)ethanone. 93% yield, obtained as a yellowish solid. M.p.: 156.9 – 158.9 °C. ^{1}H NMR (250 MHz, acetone-d_6, 2.05 ppm): δ 9.47 (s, 1H), 9.20 (d, J = 1.6 Hz, 1H), 8.52 (dd, J = 4.8 Hz, 1.6 Hz, 1H), 8.27 (dt, J = 7.6 Hz, 1.9 Hz, 1H), 7.62 (t, J = 2.0 Hz, 1H), 7.41 (dd, J = 8.2 Hz, 4.7 Hz, 1H), 7.26–7.19 (m, 2H), 7.35 (s, 1H), 6.60 (dt, J = 7.6 Hz, 1.9 Hz, 1H), 3.83 (s, 3H). ^{13}C NMR (62.5 MHz, acetone-d_6, 29.84 ppm): δ 164.8, 161.4, 149.4, 149.0, 148.3, 143.3, 133.5, 131.4, 130.6, 124.3, 110.5, 108.2, 104.6, 104.1, 55.4. HRMS (ESI +): *m/z* calculated for $C_{15}H_{14}N_3OS^+$ [M + H^+] 284.08521, found 284.08500. HPLC purity: 99%.

4-(2-((4-fluorophenyl)amino)thiazol-4-yl)benzonitrile (C12.30)

Prepared according to the general procedure for the synthesis of the aminothiazoles using 1-(4-fluorophenyl)thiourea and 4-(2-bromoacetyl) benzonitrile. 81% yield, obtained as a white solid. M.p.: 151.8 – 153.5 °C. ^{1}H NMR (250 MHz, $CDCl_3$, 7.26 ppm): δ 7.92 (d, J = 8.5 Hz, 2H), 7.66 (d, J = 8.5 Hz, 2H), 7.45 – 7.37 (m, 2H), 7.14 – 7.00 (m, 2H), 6.94 (s, 1H). ^{13}C NMR (62.5 MHz, $CDCl_3$, 77.16 ppm): δ 165.8, 159.3 (d, J = 243.5 Hz), 149.4, 138.4, 136.2 (d, J = 2.6 Hz), 132.6, 126.6, 121.1 (d, J = 8.0 Hz), 119.1, 116.3 (d, J = 22.7 Hz), 111.1, 104.9. HRMS (ESI +): *m/z* calculated for $C_{16}H_{11}FN_3S^+$ [M + H^+] 296.06522, found 296.06498. HPLC purity: 98%.

4-(2-((3,5-bis(trifluoromethyl)phenyl)amino)thiazol-4-yl)benzonitrile (C12.31)

Prepared according to the general procedure for the synthesis of the aminothiazoles using 1-(3,5-bis(trifluoromethyl)phenyl)thiourea and 4-(2-bromoacetyl)benzonitrile. 81% yield, obtained as a white solid. M.p.: 248.2 – 249.6 °C. ^{1}H NMR (250 MHz, DMSO-d_6, 2.5 ppm): δ 11.03 (s, 1H), 8.35 (s, 2H), 7.99 (d, J = 8.3 Hz, 2H), 7.84 (d, J = 8.3, 2H), 7.73 (s, 1), 7.54 (s, 1H). ^{13}C NMR (62.5 MHz, DMSO-d_6, 39.52 ppm): δ 162.4, 148.2, 142.3, 138.1, 132.7, 130.9 (q, $J_{C\text{-}F}$ = 32.5 Hz), 125.9, 123.3 (q, $J_{C\text{-}F}$ = 271.2 Hz), 118.8, 116.3 (d, $J_{C\text{-}F}$ = 3.7 Hz), 113.5–113.4 (m, 1C), 109.9, 108.4. ^{19}F NMR (235 MHz, DMSO-d_6): δ −61.8. HRMS (ESI +): *m/z* calculated for $C_{18}H_{10}F_6N_3S^+$ [M + H^+] 414.0494, found 414.0505. HPLC purity: 99%.

C12.16 analogue synthesis

To a 25 mL round bottomed flask containing 10 mL of ethanol were added compound **C12.4** (1 mmol) and $SnCl_2{\cdot}2H_2O$ (5 mmol). This suspension was heated under reflux for 3 h. After TLC showed the reaction ended, the flask was cooled and its pH neutralized with 20 mL of saturated $NaHCO_3$ aqueous solution. The resulting aqueous suspension was vacuum filtered and the filtered solution was extracted with ethyl acetate (5x10 mL). Then, the organic phase was dried over anhydrous Na_2SO_4 and evaporated under reduced pressure. The resulting crude product containing intermediate **3a** was used in the next reaction without further purification.

Next, compound **3a** (0,5 mmol) and 4 mL of anhydrous triethylamine were added to a 10 mL round bottomed flask. The flask atmosphere was exchanged to N_2. Then the flask was cooled in an ice bath and phenylacetyl chloride (0,75 mmol) was added dropwise during 20 min. The reaction mixture was stirred for 4 h at 25 °C. After completion, 5 mL of distilled water were added and the resulting aqueous phase was extracted with ethyl acetate (5x10 mL). The organic phase was then washed with 1 M HCl aqueous solution (3x10mL), 20 mL of saturated $NaHCO_3$ aqueous solution, 20 mL of brine and dried over anhydrous Na_2SO_4. The organic solvent was evaporated under reduced pressure to obtain **C12.16**, which could be used without any further purification.

N-(4-(2-((3-methoxyphenyl)amino)thiazol-4-yl)phenyl)-2-phenylacetamide (C12.16).

71% yield, obtained as slightly reddish solid. M.p.: 203.1 – 204.9 °C. ^{1}H NMR (250 MHz, Acetone-d_6, 2.05 ppm): δ 9.38 (s, 1H), 9.31 (s, 1H), 7.90 (d, J = 8.6 Hz, 2H), 7.71 (d, J = 8.6 Hz, 2H), 7.64 (s, 1H), 7.41–7.20 (m, 7H), 7.08 (s, 1H), 6.57 (dt, J = 7.1, 2.3 Hz, 1H), 3.83 (s, 3H), 3.71 (s, 2H). ^{13}C NMR (62.5 MHz, acetone-d_6, 29.84 ppm): δ 163.3, 160.5, 150.8, 142.6, 138.9, 135.9, 129.6, 129.1, 128.3, 126.6, 126.2, 119.1, 119.0, 109.5, 107.1, 103.0, 101.0, 54.5, 43.8. HRMS (ESI +): *m/z* calculated for $C_{24}H_{22}N_3O_2S^+$ [M + H^+] 416.1427, found 416.1430. HPLC purity: 95%.

C12.17 analogue synthesis

4-Phenylthiazol-2-amine (3b) [65].

Prepared according to the general procedure for the synthesis of the aminothiazoles using thiourea and 2-bromoacetophenone. Purified by recrystallization from 1:1 water/ethanol solution. 97% yield, obtained as a white solid. ^{1}H NMR (250 MHz, DMSO-d_6, 2.50 ppm): δ 8.78 (s, 2H), 7.73 (d, J = 6.6 Hz, 2H), 7.53–7.43 (m, 3H), 7.25 (s, 1H). ^{13}C NMR (62.5 MHz, DMSO-d_6, 39.52 ppm): δ 170.2, 139.4, 129.3, 129.0, 128.9, 125.8, 102.8. NMR data matches the literature.

Next, phenylacetic acid (1.5 mmol) and EDC (1 mmol) solubilized in anhydrous THF, were added to a 10 mL reaction flask containing a nitrogen atmosphere. Then, a THF solution containing compound **3b** (1 mmol) and DMAP (0.15 mmol) was added to the same reaction flask. The resulting solution was stirred for 16 h at 25 °C. After completion of the reaction, 15 mL of distilled water were added and the resulting aqueous phase was extracted with ethyl acetate (5x10 mL). The combined organic phase was washed with 20 mL of saturated $NaHCO_3$ aqueous solution, followed by 20 mL of 1 M HCl aqueous solution, 20 mL of brine and then dried over anhydrous Na_2SO_4. The organic solvent was evaporated under reduced pressure to obtain **C12.17**, which could be used without any further purification.

2-phenyl-N-(4-phenylthiazol-2-yl)acetamide (C12.17) [66].

63% yield, obtained as a white solid. ^{1}H NMR (250 MHz, $CDCl_3$, 7.26 ppm): δ 10.57 (s, 1H), 7.80 (d, J = 7.1 Hz, 2H), 7.44–7.26 (m, 6H), 7.14 (s, 1H), 7.09–7.06 (m, 2H), 3.51 (s, 2H). ^{13}C NMR (62.5 MHz, $CDCl_3$, 77.16 ppm): δ 169.2, 158.9, 149.8, 134.3, 133.1, 129.4, 129.1, 129.0, 128.3, 127.7, 126.3, 108.1, 43.0. HPLC purity: 99%. NMR data matches the literature.

C12.18 analog synthesis

To a solution of 1 mmol of phenyl acetaldehyde in 10 mL of dichloromethane in a 25 mL round bottomed flask was added 0.1 mmol of (*S*)-proline. Next, 1 mmol of *N*-bromosuccinimide was added to the same solution. The reaction was left for 2 h at room temperature, then the mixture was filtered through a silica pad with dichloromethane and the solvent evaporated. The crude 2-bromo-2-phenylacetaldehyde (**2q**) obtained was used in the Hantszch reaction step without further purification.

N-(3-methoxyphenyl)-5-phenylthiazol-2-amine (C12.18)

Obtained according to the general procedure for the synthesis of the aminothiazoles using *N*-(3-methoxyphenyl)thiourea and 2-bromo-2-phenylacetaldehyde. 63% yield, obtained as a white solid. M.p.: 148.8 – 149.9 °C. ^{1}H NMR (250 MHz, $CDCl_3$, 7.26 ppm): δ 7.48 (d, J = 7.4 Hz, 2H), 7.44 (s, 1H), 7.37–7.20 (m, 5H), 6.98–6.93 (m, 2H), 6.63 (dd, J = 8.2, 1.8 Hz, 1H), 3.82 (s, 3H). ^{13}C NMR (62.5 MHz, $CDCl_3$, 77.16 ppm): δ 160.7, 141.7, 133.7, 132.0, 130.4, 129.0, 127.2, 125.7, 110.8, 106.5, 104.3, 77.3, 55.4. HRMS (ESI +): *m/z* calculated for $C_{16}H_{14}N_2OS^+$ [M + H^+] 283.08996, found 283.08975. HPLC purity: 95%.

C12.32 analogue synthesis

4-(2-aminothiazol-4-yl)benzonitrile (3c)

Prepared according to the general procedure for the synthesis of the aminothiazoles using thiourea and 4-(2-bromoacetyl)benzonitrile. 88% yield, obtained as a white solid. ^{1}H NMR (250 MHz, DMSO-d_6, 2.50 ppm): δ 7.93 (s, 4H), 7.48 (s, 1H), 5.64 (s, 2H). ^{13}C NMR (62.5 MHz, DMSO-d_6, 39.52 ppm): δ 170.0, 139.61, 134.0, 132.9, 126.4, 118.5, 111.0, 106.4.

Next, 4-fluorophenylacetic acid (1.5 mmol) and EDC (1 mmol) solubilized in anhydrous THF, were added to a 10 mL reaction flask containing a nitrogen atmosphere. Then, a THF solution containing compound **3c** (1 mmol) and DMAP (0.15 mmol) was added to the same reaction flask. The resulting solution was stirred for 16 h at 25 °C. After completion of the reaction, 15 mL of distilled water was added and the resulting aqueous phase was extracted with ethyl acetate (5x10 mL). The combined organic phase was washed with 20 mL of saturated $NaHCO_3$ aqueous solution, followed by 20 mL of 1 M HCl aqueous solution, 20 mL of brine and then dried over anhydrous Na_2SO_4. The solvent was

evaporated and the solid purified by recrystallization in EtOH:water 8:2 to obtain **C12.32**.

N-(4-(4-cyanophenyl)thiazol-2-yl)-2-(4-fluorophenyl)acetamide (C12.32)

73% yield, obtained as a white solid. M.p.: 208 – 209.9 °C. ^{1}H NMR (250 MHz, DMSO-d_6, 2.5 ppm): δ 12.57 (s, 1H), 8.06 (d, J = 8.3 Hz, 2H), 7.89–7,86 (m, 3H), 7,37 (dd, $J_{H\text{-}F}$ = 5.8, J = 8.5 Hz, 2H), 7,15 (t, $J_{H\text{-}F}$ = 8.8, J = 8.5, 2H), 3.80 (s, 2H). ^{13}C NMR (62.5 MHz, DMSO-d_6, 39.52 ppm): δ 169.7, 161.3 (d, $J_{C\text{-}F}$ = 241.2 Hz), 158.3, 147.1, 138.4, 132.8, 131.2 (d, $J_{C\text{-}F}$ = 8.12 Hz), 130.9 (d, $J_{C\text{-}F}$ = 3.1 Hz), 126.3, 118.9, 115.2 (d, $J_{C\text{-}F}$ = 21.2 Hz) 111.7, 110.0, 40.7. ^{19}F NMR (235 MHz, DMSO-d_6): δ −116.0. HRMS (ESI +): *m/z* calculated for $C_{18}H_{13}FN_3OS^+$ [M + H$^+$] 338.07579, found 338.07521. HPLC purity 99%.

C12.33 analogue synthesis

To a round bottomed flask containing 15 mL of THF was added 2 mmol of 5-amino-1,3,4-thiadiazole-2-thiol, 2.2 mmol of K_2CO_3 and 2 mmol of 4-(bromomethyl)benzonitrile. The reaction was stirred for 16 h at room temperature and then 15 mL of cold distilled water was added the flask. The precipitated solid was vacuum filtered and then recrystallized in pure ethanol to afford compound **3d**.

4-(((5-amino-1,3,4-thiadiazol-2-yl)thio)methyl)benzonitrile (3d) [68].

92% yield, obtained as a white solid. ^{1}H NMR (250 MHz, DMSO-d_6, 2.5 ppm): δ 7.78 (d, J = 8.3 Hz, 2H), 7.53 (d, J = 8.3 Hz, 2H), 7.31 (s, 2H), 4.36 (s, 2H). ^{13}C NMR (62.5 MHz, DMSO-d_6, 39.52 ppm): δ 170.1, 148.5, 143.4, 132.3, 129.9, 118.7, 110.0, 37.8. NMR data matches the literature.

Next, 4-fluorophenylacetic acid (1.5 mmol) and EDC (1 mmol) solubilized in anhydrous THF, were added to a 10 mL reaction flask containing a nitrogen atmosphere. Then, a THF solution containing compound **3d** (1 mmol) and DMAP (0.15 mmol) was added to the same reaction flask. The resulting solution was stirred for 16 h at 25 °C. After completion of the reaction, 15 mL of distilled water was added and the resulting aqueous phase was extracted with ethyl acetate (5x10 mL). The combined organic phase was washed with 20 mL of saturated $NaHCO_3$ aqueous solution, followed by 20 mL of 1 M HCl aqueous solution, 20 mL of brine and then dried over anhydrous Na_2SO_4. The solvent was evaporated and the residue purified by recrystallization in pure EtOH to obtain **C12.33**.

N-(5-((4-cyanobenzyl)thio)-1,3,4-thiadiazol-2-yl)-2-(4-fluorophenyl) acetamide (C12.33)

84% yield, obtained as a white solid. M.p.: 195.3 – 197.1 °C. ^{1}H NMR (250 MHz, DMSO-d_6, 2.5 ppm): δ 12.85 (s, 1H), 7.77 (d, J = 7.7 Hz, 2H), 7.58 (d, J = 7.7 Hz, 2H), 7.33 (t, J = 7.2 Hz, 2H), 7.14 (t, J = 7.2 Hz, 2H), 4.54 (s, 2H), 3.80 (s, 2H). ^{13}C NMR (62.5 MHz, DMSO-d_6, 39.52 ppm): δ 169.5, 161.3 (d, $J_{C\text{-}F}$ 241.2 Hz), 159.1, 157.4, 143.0, 132.4, 131.2 (d, d, $J_{C\text{-}F}$ 8.1 Hz), 130.5 (d, $J_{C\text{-}F}$ 3.1 Hz), 129.9, 118.6, 115.1 (d, $J_{C\text{-}F}$ 21.2 Hz), 110.2, 40.5, 36.8. ^{19}F NMR (235 MHz, DMSO-d_6): δ −115.8. HRMS (ESI +): *m/z* calculated for $C_{18}H_{14}FN_4OS_2^+$ [M + H$^+$] 385.05876, found 385.05806. HPLC purity: 96%.

C12.34 analogue synthesis

To an oven dried round bottomed flask containing 2 mmol of 4-aminobenzonitrile solubilized in 15 mL of dry CH_2Cl_2 was added 2.2 mmol of dry triethylamine. The reaction mixture was cooled with an ice bath and then 2 mmol of bromoacetyl bromide was added dropwise for 5 min. The ice bath was removed and the reaction was stirred for 4 h at room temperature. After completion of the reaction, 10 mL of distilled water was added and the resulting aqueous phase was extracted with ethyl acetate (5x10 mL). The combined organic phase was washed with 2x10 mL of saturated $NaHCO_3$ aqueous solution, followed by 2x10 mL of 1 M HCl aqueous solution, 2x10 mL of brine and then dried over anhydrous Na_2SO_4. The solvent was evaporated to obtain **3e**, which was used in the next reaction without further purification.

2-bromo-N-(4-cyanophenyl)acetamide (3e) [69].

78% yield, obtained as a white solid. ^{1}H NMR (250 MHz, DMSO-d_6, 2.5 ppm): δ 10.80 (s, 1H), 7.81–7.73 (m, 4H), 4.07 (s, 2H). 13C NMR (62.5 MHz, DMSO-d_6, 39.52 ppm): δ 165.6, 142.7, 133.4, 119.3, 118.9, 105.6, 30.1. NMR data matches the literature.

To a round bottomed flask containing 15 mL of THF was added 2 mmol of 5-amino-1,3,4-thiadiazole-2-thiol, 2.2 mmol of K_2CO_3 and 2 mmol of compound **3e**. The reaction was stirred for 16 h at r.t. and then 15 mL of cold distilled water was added the flask. The precipitated solid was vacuum filtered and then recrystallized in pure ethanol to obtain compound **3f**.

2-((5-amino-1,3,4-thiadiazol-2-yl)thio)-N-(4-cyanophenyl)acetamide (3f)

87% yield, obtained as white solid. M.p.: 224.9 – 226.7 °C. ^{1}H NMR (250 MHz, DMSO-d_6, 2.5 ppm): δ 10.68 (s, 1H), 7.80–7.72 (m, 4H), 7.30 (s, 2H), 4.03 (s, 2H). ^{13}C NMR (62.5 MHz, DMSO-d_6, 39.52 ppm): δ 170.0, 166.7, 149.1, 142.9, 133.4, 119.2, 119.0, 105.3, 38.7. HRMS (ESI +): *m/z* calculated for $C_{11}H_{10}N_5OS_2^+$ [M + H$^+$] 292.03213, found 292.03179.

Next, 4-fluorophenylacetic acid (1.5 mmol) and EDC (1 mmol) solubilized in anhydrous THF, were added to a 10 mL reaction flask containing a nitrogen atmosphere. Then, a THF solution containing compound **3f** (1 mmol) and DMAP (0.15 mmol) was added to the same reaction flask. The resulting solution was stirred for 16 h at 25 °C. After completion of the reaction, 15 mL of distilled water was added and the resulting aqueous phase was extracted with ethyl acetate (5x10 mL). The combined organic phase was washed with 20 mL of saturated $NaHCO_3$ aqueous solution, followed by 20 mL of 1 M HCl aqueous solution, 20 mL of brine and then dried over anhydrous Na_2SO_4. The solvent was evaporated and the solid purified by recrystallization in pure EtOH to obtain **C12.34**.

N-(4-cyanophenyl)-2-((5-(2-(4-fluorophenyl)acetamido)-1,3,4-thiadiazol-2-yl)thio)acetamide (C12.34)

73% yield, obtained as a white solid. M.p.: 229.8 – 231.2 °C. ^{1}H NMR (250 MHz, DMSO-d_6, 2.5 ppm): δ 12.83 (s, 1H), 10.74 (s, 1H), 7.79–7.71 (m, 4H), 7.34 (t, J = 7.2 Hz, 2H), 7.14 (t, J = 7.2 Hz, 2H), 4.23 (s, 2H), 3.80 (s, 2H). ^{13}C NMR (62.5 MHz, DMSO-d_6, 39.52 ppm): δ 169.6, 166.4, 161.3 (d, $J_{C\text{-}F}$ 241.2 Hz), 159.1, 157.9, 142.8, 133.4, 131.2 (d, $J_{C\text{-}F}$ 8.1 Hz), 130.5 (d, $J_{C\text{-}F}$ 3.1 Hz), 119.2, 118.9, 115.1 (d, $J_{C\text{-}F}$ 21.2 Hz), 105.3, 40.5, 38.0. HRMS (ESI +): *m/z* calculated for $C_{19}H_{15}FN_5O_2S_2^+$ [M + H$^+$] 428.0646, found 428.0653. HPLC purity: 98%.

Declaration of Competing Interest

The authors declare that they have no known competing financial interests or personal relationships that could have appeared to influence the work reported in this paper.

Data availability

Data will be made available on request.

Acknowledgments

The authors gratefully acknowledge financial support from the São Paulo Research Foundation (FAPESP) for the awards # 2014/26378-2 (JCP), 2021/06661-5 (JCP), 20/12904-5 (RVCG), 13/07600-3 (RVCG),14/15968-3 (SMGD) and 19/16351-3 (SMGD) and the fellowships 2016/09077-4 (RKEC), 21/13736-1 (BNS), and the Coordination for the Improvement of Higher Education Personnel (CAPES) (GAB, CVZN). We thank LNBio for access to core facilities (LCCMI, LPP, and LEC) and financial support. We are very grateful to Dr. Alessandra Girasole for her expert technical support.

Appendix A. Supplementary data

Supplementary data to this article can be found online at https://doi.org/10.1016/j.rechem.2023.100842.

References

[1] D. Hanahan, R.A. Weinberg, Hallmarks of cancer: the next generation, Cell 144 (5) (2011) 646–674, https://doi.org/10.1016/j.cell.2011.02.013.

[2] N.N.N.N. Pavlova, C.B.C.B. Thompson, The emerging hallmarks of cancer metabolism, Cell Metab. 23 (1) (2016) 27–47, https://doi.org/10.1016/j.cmet.2015.12.006.

[3] M.J. Lukey, W.P. Katt, R.A. Cerione, Targeting Therapy Resistance: When Glutamine Catabolism Becomes Essential, Cancer Cell 33 (5) (2018) 795–797, https://doi.org/10.1016/j.ccell.2018.04.009.

[4] Y.K. Choi, K.G. Park, Targeting Glutamine Metabolism for Cancer Treatment, Biomol Ther (Seoul). 26 (1) (2018) 19–28, https://doi.org/10.4062/biomolther.2017.178.

[5] Warburg O. On the Origin of Cancer Cells. *Science (1979)*. 1956;123(3191):309-314. 10.1126/science.123.3191.309.

[6] J. Zhu, C.B. Thompson, Metabolic regulation of cell growth and proliferation, Nat. Rev. Mol. Cell Biol. 20 (7) (2019) 436–450, https://doi.org/10.1038/s41580-019-0123-5.

[7] S. Wang, Y. Yan, W.J. Xu, et al., The Role of Glutamine and Glutaminase in Pulmonary Hypertension, Front Cardiovasc Med. (2022) 9, https://doi.org/10.3389/fcvm.2022.838657.

[8] J. Márquez, A.R. López de la Oliva, J.M. Matés, J.A. Segura, F.J. Alonso, Glutaminase: A multifaceted protein not only involved in generating glutamate, Neurochem. Int. 48 (6–7) (2006) 465–471, https://doi.org/10.1016/j.neuint.2005.10.015.

[9] R.J. DeBerardinis, N.S. Chandel, Fundamentals of cancer metabolism. *Sci Adv*. 2 (5) (2016) e1600200.

[10] L. Yang, S. Venneti, D. Nagrath, Glutaminolysis: A hallmark of cancer metabolism, Annu. Rev. Biomed. Eng. 19 (1) (2017) 163–194, https://doi.org/10.1146/annurev-bioeng-071516-044546.

[11] T.Q. Tran, X.H. Lowman, M. Kong, Molecular pathways: metabolic control of histone methylation and gene expression in cancer, Clin. Cancer Res. 23 (15) (2017) 4004–4009, https://doi.org/10.1158/1078-0432.CCR-16-2506.

[12] Z. Wang, F. Liu, N. Fan, et al., Targeting glutaminolysis: new perspectives to understand cancer development and novel strategies for potential target therapies, Front. Oncol. (2020) 10, https://doi.org/10.3389/fonc.2020.589508.

[13] C.C. Pasquali, Z. Islam, D. Adamoski, et al., The origin and evolution of human glutaminases and their atypical C-terminal ankyrin repeats, J. Biol. Chem. 292 (27) (2017) 11572–11585, https://doi.org/10.1074/jbc.M117.787291.

[14] B.K. Masisi, R. El Ansari, L. Alfarsi, E.A. Rakha, A.R. Green, M.L. Craze, The role of glutaminase in cancer, Histopathology 76 (4) (2020) 498–508, https://doi.org/10.1111/his.14014.

[15] A. Cassago, A.P.S. Ferreira, I.M. Ferreira, et al., Mitochondrial localization and structure-based phosphate activation mechanism of Glutaminase C with implications for cancer metabolism, PNAS 109 (4) (2012) 1092–1097, https://doi.org/10.1073/pnas.1112495109.

[16] M. Martín-Rufián, M. Tosina, J.A. Campos-Sandoval, et al., Mammalian glutaminase Gls2 gene encodes two functional alternative transcripts by a surrogate promoter usage mechanism, PLoS One 7 (6) (2012), https://doi.org/10.1371/journal.pone.0038380.

[17] E. Costa RK, C.T. Rodrigues, H. Campos JC, et al., High-throughput screening reveals new glutaminase inhibitor molecules, ACS Pharmacol Transl Sci. 4 (6) (2021) 1849–1866, https://doi.org/10.1021/acsptsci.1c00226.

[18] H. Yao, G. He, S. Yan, et al., Triple-negative breast cancer: is there a treatment on the horizon? Oncotarget 8 (1) (2017) 1913–1924, https://doi.org/10.18632/oncotarget.12284.

[19] M. Lampa, H. Arlt, T. He, et al., Glutaminase is essential for the growth of triple-negative breast cancer cells with a deregulated glutamine metabolism pathway and its suppression synergizes with mTOR inhibition, PLoS One 12 (9) (2017), https://doi.org/10.1371/journal.pone.0185092. Tan M, ed e0185092.

[20] G.B. Magill, W.P.L. Myers, H.C. Reilly, et al., Pharmacological and initial therapeutic observations on 6-Diazo-5-Oxo-L-Norleucine (Don) in human neoplastic disease, Cancer 10 (6) (1957) 1138–1150, https://doi.org/10.1002/1097-0142(195711/12)10:6<1138::AID-CNCR2820100608>3.0.CO;2-K.

[21] R.W. Newcomb, Selective inhibition of glutaminaseby bis-thadiazoles, Published online, 2002, 14.

[22] D.N. Edwards, V.M. Ngwa, A.L. Raybuck, et al., Selective glutamine metabolism inhibition in tumor cells improves antitumor T lymphocyte activity in triple-negative breast cancer, J. Clin. Investig. 131 (4) (2021), https://doi.org/10.1172/JCI140100.

[23] X. Sun, M. Wang, M. Wang, et al., Metabolic reprogramming in triple-negative breast cancer, Front Oncol. (2020) 10, https://doi.org/10.3389/fonc.2020.00428.

[24] B. Li, Y. Cao, G. Meng, et al., Targeting glutaminase 1 attenuates stemness properties in hepatocellular carcinoma by increasing reactive oxygen species and suppressing Wnt/beta-catenin pathway, EBioMedicine 39 (2019) 239–254, https://doi.org/10.1016/j.ebiom.2018.11.063.

[25] A.P.S. Ferreira, A. Cassago, K. de A Gonçalves, et al., Active glutaminase C Self-assembles into a supratetrameric oligomer that can be disrupted by an allosteric inhibitor, J. Biol. Chem. 288 (39) (2013) 28009–28020, https://doi.org/10.1074/jbc.M113.501346.

[26] M.M. Robinson, S.J. McBryant, T. Tsukamoto, et al., Novel mechanism of inhibition of rat kidney-type glutaminase by bis-2-(5-phenylacetamido-1,2,4-thiadiazol-2-yl)ethyl sulfide (BPTES), Biochem. J 406 (3) (2007) 407–414, https://doi.org/10.1042/BJ20070039.

[27] K. Thangavelu, C.Q. Pan, T. Karlberg, et al., Structural basis for the allosteric inhibitory mechanism of human kidney-type glutaminase (KGA) and its regulation by Raf-Mek-Erk signaling in cancer cell metabolism, PNAS 109 (20) (2012) 7705–7710, https://doi.org/10.1073/pnas.1116573109.

[28] B. DeLaBarre, S. Gross, C. Fang, et al., Full-length human glutaminase in complex with an allosteric inhibitor, Biochemistry 50 (50) (2011) 10764–10770, https://doi.org/10.1021/bi201613d.

[29] X. Xu, Y. Meng, L. Li, et al., Overview of the development of glutaminase inhibitors: achievements and future directions, J. Med. Chem. 62 (3) (2019) 1096–1115, https://doi.org/10.1021/acs.jmedchem.8b00961.

[30] K. Shukla, D.V. Ferraris, A.G. Thomas, et al., Design, synthesis, and pharmacological evaluation of bis-2-(5-phenylacetamido-1,2,4-thiadiazol-2-yl) ethyl sulfide 3 (BPTES) analogs as glutaminase inhibitors, J Med Chem. 55 (23) (2012) 10551–10563, https://doi.org/10.1021/jm301191p.

[31] M.I. Gross, S.D. Demo, J.B. Dennison, et al., Antitumor activity of the glutaminase inhibitor CB-839 in triple-negative breast cancer, Mol. Cancer Ther. 13 (April) (2014) 890–901, https://doi.org/10.1158/1535-7163.MCT-13-0870.

[32] J.J. Harding, M.L. Telli, P.N. Munster, et al., Safety and tolerability of increasing doses of CB-839, a first-in-class, orally administered small molecule inhibitor of glutaminase, in solid tumors, J. Clin. Oncol. 33 (15_suppl) (2015), https://doi.org/10.1200/jco.2015.33.15_suppl.2512, 2512–2512.

[33] M.J. Soth, K. Le, M.E. Di Francesco, et al., Discovery of IPN60090, a clinical stage selective glutaminase-1 (GLS-1) inhibitor with excellent pharmacokinetic and physicochemical properties, J. Med. Chem. 63 (21) (2020) 12957–12977, https://doi.org/10.1021/acs.jmedchem.0c01398.

[34] X. Xu, J. Wang, M. Wang, et al., Structure-enabled discovery of novel macrocyclic inhibitors targeting glutaminase 1 allosteric binding site, J. Med. Chem. 64 (8) (2021) 4588–4611, https://doi.org/10.1021/acs.jmedchem.0c02044.

[35] S.K. Milano, Q. Huang, T.T.T. Nguyen, et al., New insights into the molecular mechanisms of glutaminase C inhibitors in cancer cells using serial room temperature crystallography, J. Biol. Chem. 298 (2) (2022), 101535, https://doi.org/10.1016/j.jbc.2021.101535.

[36] S.C. Zimmermann, B. Duvall, T. Tsukamoto, Recent progress in the discovery of allosteric inhibitors of kidney-type glutaminase, J. Med. Chem. 62 (1) (2019) 46–59, https://doi.org/10.1021/acs.jmedchem.8b00327.

[37] E. Garcia-Egido, S.Y.F. Wong, B.H. Warrington, A Hantzsch synthesis of 2-amino-thiazoles performed in a heated microreactor system, Lab Chip 2 (1) (2002) 31, https://doi.org/10.1039/b109360f.

[38] M. Farouk Elsadek, B. Mohamed Ahmed, F.M. Fawzi, An overview on synthetic 2-aminothiazole-based compounds associated with four biological activities, Molecules 26 (5) (2021) 1449, https://doi.org/10.3390/molecules26051449.

[39] M.R. Maddani, K.R. Prabhu, A concise synthesis of substituted thiourea derivatives in aqueous medium, J. Org. Chem. 75 (7) (2010) 2327–2332, https://doi.org/10.1021/jo1001593.

[40] M.M. Ansari, S.P. Deshmukh, R. Khan, M. Musaddiq, Synthesis antimicrobial and anticancer evaluation of 1-Aryl-5-(o -methoxyphenyl)-2- S -benzyl isothiobiurets, Int J Med Chem. 2014 (2014) 1–5, https://doi.org/10.1155/2014/352626.

[41] K. Jeong Wan, Lee J. Hun, Park S. Mi, et al., Synthesis and in-vitro evaluation of 2-amino-4-arylthiazole as inhibitor of 3D polymerase against foot-and-mouth disease (FMD), Eur J Med Chem. 102 (2015) 387–397, https://doi.org/10.1016/j.ejmech.2015.08.020.

[42] C.C. Fjeld, W.T. Birdsong, R.H. Goodman, Differential binding of NAD+ and NADH allows the transcriptional corepressor carboxyl-terminal binding protein to serve as a metabolic sensor, Proc. Natl. Acad. Sci. 100 (16) (2003) 9202–9207, https://doi.org/10.1073/pnas.1633591100.

[43] Dias MM, Adamoski D, Reis LM, et al. GLS2 is protumorigenic in breast cancers. *Oncogene*. 10.1038/s41388-019-1007-z.

[44] E. Costa RK. Development of New Inhibitors of the Glutaminase Enzyme with Potential Antitumor Action. State University of Campinas; 2021.

[45] M.M. Dias, D. Adamoski, L.M. dos Reis, et al., GLS2 is protumorigenic in breast cancers, Oncogene 39 (3) (2020) 690–702, https://doi.org/10.1038/s41388-019-1007-z.

[46] R. Subramanian, M.R. Lee, J.G. Allen, et al., Cytochrome P450-Mediated Epoxidation of 2-Aminothiazole-Based AKT Inhibitors: Identification of Novel GSH Adducts and Reduction of Metabolic Activation through Structural Changes Guided by in Silico and in Vitro Screening, Chem. Res. Toxicol. 23 (3) (2010) 653–663, https://doi.org/10.1021/tx900414g.

[47] S.R. Alizadeh, S.M. Hashemi, Development and therapeutic potential of 2-amino-thiazole derivatives in anticancer drug discovery, Med. Chem. Res. 30 (4) (2021) 771–806, https://doi.org/10.1007/s00044-020-02686-2.

[48] D. Das, P. Sikdar, M. Bairagi, Recent developments of 2-aminothiazoles in medicinal chemistry, Eur. J. Med. Chem. 109 (2016) 89–98, https://doi.org/10.1016/j.ejmech.2015.12.022.

[53] Ritz C, Baty F, Streibig JC, Gerhard D. Dose-Response Analysis Using R. Xia Y, ed. *PLoS One*. 2015;10(12):e0146021. 10.1371/journal.pone.0146021.

[54] C. Elgert, A. Rühle, P. Sandner, S. Behrends, Thermal shift assay: Strengths and weaknesses of the method to investigate the ligand-induced thermostabilization of soluble guanylyl cyclase, J. Pharm. Biomed. Anal. 181 (2020), 113065, https://doi.org/10.1016/j.jpba.2019.113065.

[55] S. Majnooni, J. Duffield, J. Price, A.R. Khosropour, H. Zali-Boeini, H. Beyzavi, Aryliodoazide Synthons: A Different Approach for Diversified Synthesis of 2-Aminothiazole, 1,3-Thiazole, and 1,3-Selenazole Scaffolds, ACS Comb. Sci. 21 (7) (2019) 516–521, https://doi.org/10.1021/acscombsci.9b00045.

[56] S. Heng, K.R. Gryncel, E.R. Kantrowitz, A library of novel allosteric inhibitors against fructose 1,6-bisphosphatase, Bioorg. Med. Chem. 17 (11) (2009) 3916–3922, https://doi.org/10.1016/j.bmc.2009.04.030.

[57] Z.H. Zhang, Y. Chen, X.J. Yan, et al., Synthesis and evaluation of novel urea and amide derivatives of 2-amino-4-phenylthiazole as potential antibacterial agents,

Med. Chem. Res. 26 (9) (2017) 2080–2087, https://doi.org/10.1007/s00044-017-1910-1.

[58] C.B. Rödl, D. Vogt, S.B.M. Kretschmer, et al., Multi-dimensional target profiling of N,4-diaryl-1,3-thiazole-2-amines as potent inhibitors of eicosanoid metabolism, Eur. J. Med. Chem. 84 (2014) 302–311, https://doi.org/10.1016/j.ejmech.2014.07.025.

[59] M. Pieroni, B. Wan, S. Cho, S.G. Franzblau, G. Costantino, Design, synthesis and investigation on the structure–activity relationships of N-substituted 2-aminothiazole derivatives as antitubercular agents, Eur. J. Med. Chem. 72 (2014) 26–34, https://doi.org/10.1016/j.ejmech.2013.11.007.

[60] M.P. Alam, T. Bilousova, P. Spilman, et al., A Small Molecule Mimetic of the Humanin Peptide as a Candidate for Modulating NMDA-Induced Neurotoxicity, ACS Chem. Nerosci. 9 (3) (2018) 462–468, https://doi.org/10.1021/acschemneuro.7b00350.

[61] K.K. Roy, S. Singh, S.K. Sharma, R. Srivastava, V. Chaturvedi, A.K. Saxena, Synthesis and biological evaluation of substituted 4-arylthiazol-2-amino derivatives as potent growth inhibitors of replicating Mycobacterium tuberculosis H37RV, Bioorg. Med. Chem. Lett. 21 (18) (2011) 5589–5593, https://doi.org/10.1016/j.bmcl.2011.06.076.

[62] Dighe SN, Chaskar PK, Jain KS, Phoujdar MS, Srinivasan K v. A Remarkably High-Speed Solution-Phase Combinatorial Synthesis of 2-Substituted-Amino-4-Aryl Thiazoles in Polar Solvents in the Absence of a Catalyst under Ambient Conditions and Study of Their Antimicrobial Activities. *ISRN Org Chem.* 2011;2011:1-6. 10.5402/2011/434613.

[63] K.S. Jain, J.B. Bariwal, M.K. Kathiravan, et al., An efficient and rapid synthesis of 2-amino-4-arylthiazoles employing microwave irradiation in water, Green Sustainable Chem. 01 (02) (2011) 35–38, https://doi.org/10.4236/gsc.2011.12007.

[64] D.S. Wagare, P.D. Netankar, M. Shaikh, M. Farooqui, A. Durrani, Highly efficient microwave-assisted one-pot synthesis of 4-aryl-2-aminothiazoles in aqueous medium, Environ. Chem. Lett. 15 (3) (2017) 475–479, https://doi.org/10.1007/s10311-017-0619-1.

[65] L. Guo, B. Yan, Chemical-bonding assembly, physical characterization, and photophysical properties of lanthanide hybrids from a functional thiazole bridge, Eur. J. Inorg. Chem. 2010 (8) (2010) 1267–1274, https://doi.org/10.1002/ejic.200901006.

[66] J.R. Li, D.D. Li, R.R. Wang, et al., Design and synthesis of thiazole derivatives as potent FabH inhibitors with antibacterial activity, Eur. J. Med. Chem. 75 (2014) 438–447, https://doi.org/10.1016/j.ejmech.2013.11.020.

[68] P.M. Wehrli, I. Uzelac, T. Olsson, T. Jacso, D. Tietze, J. Gottfries, Discovery and development of substituted thiadiazoles as inhibitors of Staphylococcus aureus Sortase A, Bioorg. Med. Chem. 27 (19) (2019), 115043, https://doi.org/10.1016/j.bmc.2019.115043.

[69] S.J. Ratnakar, M. Woods, A.J.M. Lubag, Z. Kovács, A.D. Sherry, Modulation of water exchange in europium(III) DOTA−tetraamide complexes via electronic substituent effects, J. Am. Chem. Soc. 130 (1) (2008) 6–7, https://doi.org/10.1021/ja076325y.